肝臓　49巻4号　145–152（2008）

＜原　著＞

1b型高ウイルス量高齢者C型慢性肝炎に対するPEG IFNα-2b/リバビリン治療（併用療法）の検討

金　守良[1]*　井本　勉[1]　婦木　秀一[1]　金　啓二[2]
谷口　美幸[3]　長野　基子[4]　堀田　博[4]　勝二　郁夫[4]
寒原　芳浩[5]　前川　陽子[6]　工藤　正俊[7]　林　祥剛[8]

要旨：1b型高ウイルスC型慢性肝炎の65歳以上（高齢群）23名（平均年齢69.4歳）と65歳未満（非高齢群）52名（平均年齢53.5歳）を対象にIFNα2b/リバビリン併用療法を比較検討した．著効率と中断率は高齢群37.5%（6/16），30.4%（7/23），非高齢群50%（20/40），23.1%（12/52）で有意差はなく，HCVコア抗原減少率，2-5AS応答率も両群間に有意差を認めなかった．高齢群では著効例は非著効例に比して開始時のAFP値が有意に低値であった（P<0.01）．高齢群では著効・非著効を問わず治療前後でAFP値は有意に低下しており（開始時10.1±9.55 ng/ml，終了時5.18±4.52 ng/ml（P<0.05）），治療により発癌抑制がもたらされた可能性が考えられた．よって，高齢群においては，たとえ著効に至らない場合であっても治療の完遂が重要である．

索引用語：1b型高ウイルス量C型慢性肝炎　PEG IFNα-2b/リバビリン併用療法　高齢者　発癌抑制　AFP

緒　言

C型慢性肝炎は肝硬変や肝癌に進展する重篤な疾患である．近年，C型慢性肝炎の高齢化が顕著であり[1]，それに伴って肝癌発生も高齢化する傾向にあり，肝癌好発年齢は60歳代になっている[2]．一方，適切なIFN治療によりC型慢性肝炎の治療がなされ著効に持ち込めれば，肝発癌率を低下させることが示されている[3]．C型肝炎のゲノタイプについていえば，日本においては70%が1b型で，残りの30%が2a，2b型である．1b型のうち，70%が高ウイルス量の患者である[4]．こうした1b型高ウイルス量の患者に対して，従来のIFN単独療法は10%以下の低い著効率しかもたらさなかった[5]．

IFN治療の進歩，すなわちPEG IFNα-2b/リバビリン治療（併用療法）は1b型高ウイルス量患者においても50～60%の高い著効率をもたらしている[6][7]．ただ，1b型高ウイルス量患者に対するこの併用療法においても，インスリン抵抗性[8][9]，肝脂肪化[10]，肝線維化の進んだ症例，肥満例，女性，高齢者などで著効率が低い傾向にある[8]．しかし，1b型高ウイルス量高齢者C型慢性肝炎に対する併用療法に関してその著効率，著効に関する因子，及び発癌抑制の検討は少ない．

この併用療法のもう一つの問題点はPEG IFNα-2b投与による食欲不振，全身倦怠，血球減少の副作用に加えて，リバビリン投与による貧血などの副作用が顕著なこと，とりわけ高齢者においてその副作用のために治療の継続を困難にしていることである[11]～[13]．ただ，その中断時期，中断率，中断理由の検討は少ない．そこで，1b型高ウイルス量高齢者C型慢性肝炎に対する併用療法の現状を把握する目的で65歳以上の高齢者の症例を65歳未満の症例と比較した．

1）神戸朝日病院消化器科
2）神戸朝日病院薬剤部
3）神戸朝日病院地域医療連携室
4）神戸大学大学院微生物学
5）兵庫県立がんセンター外科
6）順心病院外科
7）近畿大学消化器内科
8）神戸大学大学院遺伝病統御学分野
*Corresponding author: asahi-hp@arion.ocn.ne.jp

＜受付日2007年8月3日＞＜採択日2008年2月28日＞

Table 1 Host-dependent, virus related profile in the Elderly and Non-Elderly group

group	Elderly group	Non-Elderly group	*P*-value
Gender (M/F)	10/6	23/17	0.73
IFN treatment (retrial/naive)	4/9	22/17	0.11
HCV RNA level (KIU/mL)	2069±1380	1727±1581	0.35
HCV core antigen (fmol/L)	11058±13549	7256±7634	0.10
AST (IU/L)	40.4±19.4	46.3±33.7	0.96
ALT (IU/L)	39.8±19.9	52.9±38.0	0.39
Hb (g/dL)	13.7±1.39	13.9±1.65	0.93
WBC (/μL)	53.0±21.0	45.8±11.9	0.28
PLT (10^4/μL)	16.5±6.45	15.6±4.93	0.77
AFP (ng/mL)	10.1±9.55	12.0±29.9	0.30
HOMA-IR	11.5±17.5	5.70±5.63	0.20
BMI (%)	23.5±4.21	22.3±3.71	0.31
F0, 1/F2, 3	3/9	20/12	0.03

対象と方法

対象は，当院でPEG IFNα-2b/リバビリンの併用療法を48週行ない，2007年4月までに治療を終了した1b型高ウイルス量（HCV RNA定量ハイレンジ法で100 KIU/ml以上）C型慢性肝炎患者75名である．65歳以上の症例（以下，高齢群）23名（65歳～75歳　平均69.4歳　男性14名，女性9名），65歳未満の症例（以下，非高齢群）52名（28歳～64歳　平均53.5歳　男性33名，女性19名）である．両群間の患者背景をTable 1に記した．まず両群の著効率を検討した．著効とは，併用療法終了後6カ月においてもHCV-RNA陰性症例と定義した．又，全症例についてウイルスダイナミックスのマーカーとしてのHCVコア抗原減少率（測定時HCVコア抗原量/併用療法投与前　HCVコア抗原量）を24時間後，1週，2週，4週後に測定した．

HCVコア抗原量はIRMA法（fmol/L）（Ortho Clinical Diagnostics, Tokyo, Japan）で測定した．IFN誘導蛋白としての2-5AS（オリゴアデニレートシンゼターゼ）の応答率（測定時2-5AS量/併用療法投与前2-5AS量）を2，8，12，24，48週で測定した．2-5ASはRIA法（pmol/dL）（Eiken Immunochemical Laboratory, Tokyo, Japan）で測定した．治療前後のAFP値（ng/ml）を検討した．血球減少率はHb，白血球，血小板の減少率を4週から48週まで4週毎に測定した．治療を完遂した例について，PEG IFNα-2b及びリバビリンの減量症例数を検討した．治療を中断した症例について，両群とも中断症例数と中断した時期，中断の理由を検討した．

結　果

患者背景で高齢群で線維化が進行していたが（P＝0.03），それ以外の初回治療例の割合，男女比，HCV RNA量，HCVコア抗原量，AST値，ALT値，Hb値，白血球数，血小板数，AFP値，HOMA-IR，BMIでは両群間に差はなかった（Table 1）．著効率では，高齢群では37.5%（6/16），非高齢群では50%（20/40）で，統計学的に有意差はみられなかった（Fig. 1）．又，高齢群では男性の著効率は50%（3/6），女性は50%（3/6），性差はなく，非高齢群でも男性の著効率は65%（13/20）で女性は35%（7/20）で性差はなかった（P＝0.058）．

開始時と24時間後，1，2，4週後におけるコア抗原減少率においては，24時間後において高齢群でやや低い傾向はあったが（P＝0.069），1，2，4週間後では有意差はみられなかった（Fig. 2）．2-5AS応答率のデーターでは，いずれの時点でも両群間に有意差は認めなかった（Fig. 3）．

又，高齢群は著効例（AFP3.97±1.84 ng/ml）が非著効例（14.1±10.6 ng/ml）に比して開始時のAFP値が有意に低値であった（P＜0.01）（Fig. 4）．非高齢群では開始時のAFP値は著効例（5.27±4.08 ng/ml）と非著効例（18.7±41.6 ng/ml）との間に有意差はなかった（P＝0.125）．高齢群ではAFP値は治療前後で有意な低下がみられ（開始時10.1±9.55 ng/ml，終了時5.18±4.52 ng/ml）（P＜0.05），著効例（開始時3.97±1.84 ng/ml，

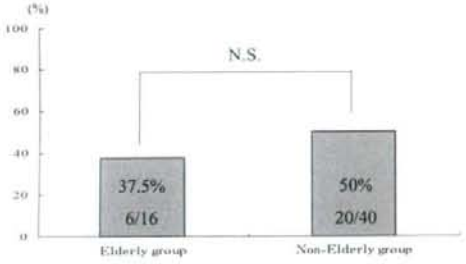

Fig. 1 The rate of sustained virologic response

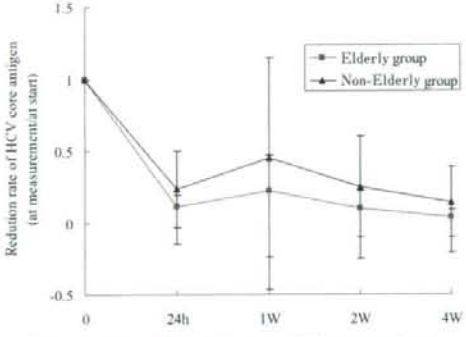

Fig. 2 The reduction rate of HCV core antigen

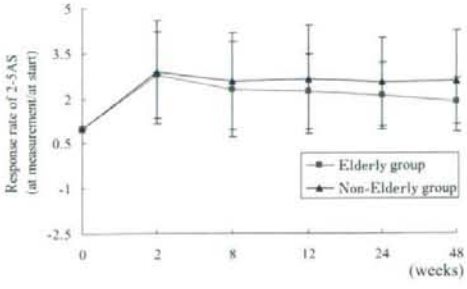

Fig. 3 The response rate of 2-5AS

終了時 2.90±1.06 ng/ml) のみならず (P<0.05)，非著効例 (開始時 14.1±10.6 ng/ml，終了時 6.11±5.33 ng/ml) においてもみられた (P<0.05) (Fig. 4，Fig. 5)．非高齢群は開始時 AFP 値 12.0±29.9 ng/ml であったが，終了時 10.5±24.7 ng/ml で治療前後で有意差はなかった

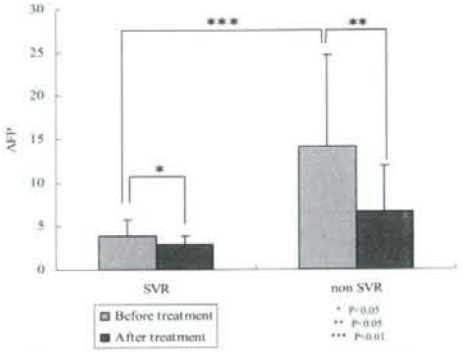

Fig. 4 The change of AFP values in the Elderly group

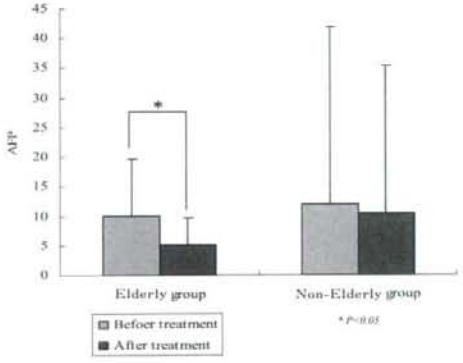

Fig. 5 The change of AFP values in the Elderly and Non-Elderly group

(P=0.052) (Fig. 5)．治療開始時から 4 週間毎の Hb 量の減少率では，20 週で高齢群 (高齢群減少率 (0.72±0.077)) は，非高齢群 (非高齢群減少率 (0.78±0.093)) と比較して有意に低下していたが (P=0.033)，その他のいずれの時点でも両群間において差はなかった (Fig. 6)．白血球数の減少率では，いずれの時点でも両群間に有意差はみられなかった (Fig. 7)．血小板数の減少率についても，いずれの時点でも両群間で有意差はみられなかった (Fig. 8)．

治療を完遂した症例で，PEG IFNα-2b を減量した症例は全体で 4 例あり，高齢 16 例中 1 例 (6.2%)，非高齢群 40 例中 3 例 (7.5%) で両群間に差はなかった．

治療を完遂した症例で，リバビリンを減量した症例

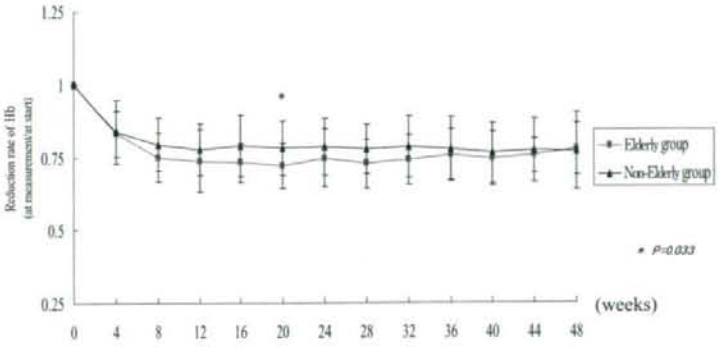

Fig. 6　The reduction rate of hemoglobin

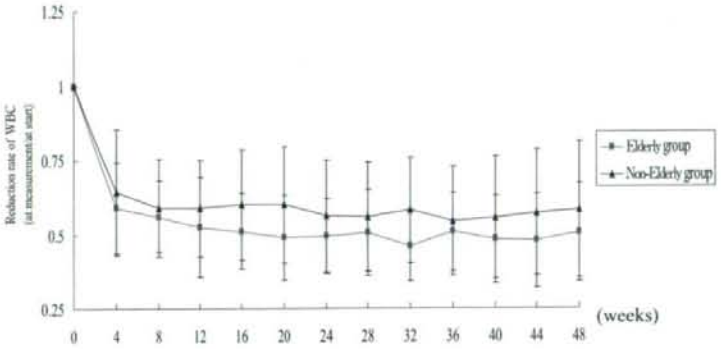

Fig. 7　The reduction rate of white blood cells

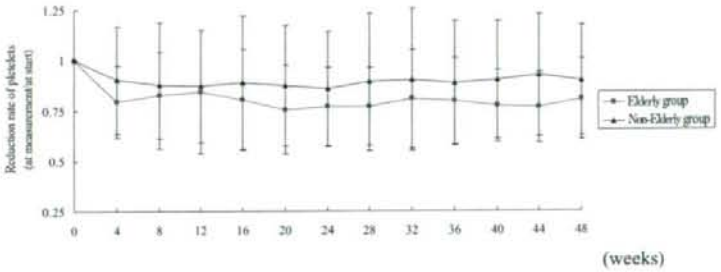

Fig. 8　The reduction rate of platelets

は全体で13例あり，高齢群16例中3例（18.8%），非高齢群40例中10例（25%）で両群間に差はなかった．治療を中断した19例について検討したところ，高齢群は23例中7例(30.4%)，非高齢群は52例中12例(23.1%)で，両群間で中断率に差はみられなかった．治療を中断した理由として，高齢群は4週以内に4例57%（4/7)で，血小板数減少1例，発熱1例，全身倦怠2例．8週以内に全身倦怠1例で，20週以内に自己中断1例

Table 2 The cases of discontinuation

Elderly group		
4 weeks after therapy	4 cases	thrombocytopenia (1 case)
		high fever (1 case)
		general fatigue (2 cases)
8 weeks after therapy	1 case	general fatigue
20 weeks after therapy	1 case	self-discontinuation
45 weeks after therapy	1 case	interstitial pneumonia
Non-Elderly group		
4 weeks after therapy	5 cases	depression (1 case)
		self-discontinuation (2 cases)
		general fatigue (1 case)
		another disease (1 case)
8 weeks after therapy	3 cases	another disease (1 case)
		self-discontinuation (2 cases)
20 weeks after therapy	2 cases	self-discontinuation
24 weeks after therapy	2 cases	another disease (1 case)
		interstitial pneumonia (1 case)

で，45週に間質性肺炎1例であった．非高齢群は4週以内に5例41.7%(5/12)で，うつ症状が1例，自己中断が2例，全身倦怠が1例，他疾患治療が1例，8週以内に3例で，他疾患治療1例，自己中断2例，20週以内に自己中断が2例，24週以内に2例で，他疾患治療1例，間質性肺炎1例であった（Table 2）．

考　察

患者背景で線維化が高齢群に進行していた．初回治療例の割合，男女比，HCV RNA量，HCVコア抗原量，AST値，ALT値，Hb値，白血球数，血小板数，AFP値，HOMA-IR，BMI，に両群間に差はなかった．併用療法のこれまでの治療成績をみると著効率に与える宿主因子として肝病理組織の脂肪化，線維化，閉経後の女性などの因子とともに高齢化が挙げられている[10]．しかし，我々の検討では著効率は高齢群と非高齢群との間に統計的には有意差はみられなかった．その原因として，今回の我々の検討では症例数が少なく，small groupによる検討であったことが関係している可能性がある．

又，高齢群と非高齢群との間に著効率に有意差がみられなかった要因としてウイルスダイナミックスのマーカー[11]としてのHCV抗原減少率[12～16]とIFN誘導蛋白の動態としての2-5AS応答率[15,17]とが両群間で同様な傾向を示し有意差を示さなかったことが挙げられる．C型慢性肝炎のIFN治療においてウイルスダイナミックスについてはIFNが直接肝細胞に働いて抗ウイルス蛋白を合成し，その作用により24時間以内でウイルスが急速に減少する投与後24時間までの第1期と，次いで上記の直接の抗ウイルス作用と細胞障害性Tリンパ球の働きによってC型肝炎ウイルス感染肝細胞が排除される投与後24時間から2週間までの第2期に分けられる[18,20,21]．1期，2期のいずれの時期においても高齢群と非高齢群においてウイルスダイナミックスすなわちHCV抗原減少率において差はみられなかった[19]．

2-5ASはIFNを投与された細胞で発見されたウイルスの増殖に必要な蛋白の阻害酵素であり，IFNの抗ウイルス活性と関係していることが確認された[22,23]．その後，2-5ASの上昇がIFN治療効果の予測に有用であることが示された[24～26]．ただ，今回の我々の検討では，2-5AS応答率はいずれの時点でも高齢群と非高齢群において差はみられなかった．

開始前のAFP値については高齢群と非高齢群の間に差はなかった．高齢群では治療前後でAFP値の低下がみられた．しかもそれは著効例のみならず，非著効例においてもみられた．非高齢群では治療前後にAFP値の有意の低下はみられていない．高齢群にみられた併用療法による治療前後のAFP値の低下がすべてIFNによる発癌抑制作用[27]によるものかどうかはにわかには断じがたい．AFP値低下が肝機能改善や線維化改善による可能性もあるからである．しかし，高齢群において併用療法の治療前後にみられたAFP値の低下は発癌抑制を何らかの形で反映していると考えてよいと思われる．それは60歳以上1b型高ウイルス量C型慢性肝炎患者の高齢者を対象としたIFN少量長期療法でAFP値が低下した症例からは発癌した症例がなかったという野村らの報告によっても支持される[28]．従って発癌抑制のためには高齢群において著効に至らなくても併用療法の完遂が重要である．又，高齢群における著効例は開始時のAFP値が非著効例に比較して有意に低値であった．芥田らは併用療法において開始前のAFP値が治療効果予測因子となること，その理由としてAFP値高値が線維化の進展を反映しているとしている[29]．今回我々の検討でも高齢群においては芥田らの報告と合致した．非高齢群では著効例と非著効例との間に開始時のAFP値に有意差はなかった．その理由は不明であるが，開始時AFP値が高齢群での治療効果予測因子の一つになることは重要な所見と考える．

我々の検討では患者背景として，高齢群はHb 13.7 g/dl，血小板16.5万/μl，白血球5300/μlであり，非高齢群はHb 13.9 g/dl，血小板15.6万/μl，白血球4580/μlで，高齢群と非高齢群では差はなかった．我々の今回の検討においては，併用療法後のHb，白血球，血小板などの血球の減少は20週目のHbが高齢群で有意に低下した以外，いずれの時点でも両群間に差はなかった．

治療を完遂した症例について，PEG IFNα-2bとリバビリンの減量率は両群間に差はなかった．このことも又，両群の著効率に差がなかった一つの要因として挙げられる．逆にいえば，高齢者のIFNとリバビリンの減量率を非高齢者と同様に抑えることができるなら，高齢群の著効率を非高齢群と同様に引き上げることができる．

中断症例についてみると，高齢群30.4%（7/23），非高齢群23.1%（12/52）と両群間に差はなかったが，その内容については差がみられた．すなわち高齢群においては4週目までは血小板数減少1例，発熱1例，全身倦怠2例で，8週目には全身倦怠1例，20週目に自己中断1例，45週目に間質性肺炎1例であった．非高齢群においては，4週以内5例で，その内容はうつ症状1例，自己中断2例，全身倦怠1例，他疾患治療1例であった．8週目までは3例で，他疾患治療1例，自己中断2例，20週目までは自己中断2例，24週目までは他疾患治療1例，間質性肺炎1例であった．特徴的なことは，65歳以上の高齢群で，開始後8週という早い時期に全身倦怠を訴えて中断した症例が中断症例5例中3例あったことである．非高齢群では，全身倦怠で中断した症例は中断症例10例中1例のみであった．高齢群の全身倦怠がリバビリンによる貧血によるものか，IFN投与による全身倦怠なのかは明らかでない．

1b型高ウイルス量高齢者C型慢性肝炎において併用療法が著効例のみならず，非著効例においても発癌抑制効果がみられたことは重要であり，治療の完遂こそが重要である．従って日常診療に従事する臨床医にあっては，高齢者の中断対策，とりわけ治療早期にみられる全身倦怠に対してきめ細かい対応が要求されている．そのことが1b型高ウイルス量高齢者C型慢性肝炎のIFN治療成績の向上及び発癌抑制につながるものと考えられる．

謝辞：本論文作成にあたり，御協力頂きました神戸朝日病院文書課・宮内　美奈子氏，川村　佳子氏，同薬剤部・笹瀬　典子氏，神戸薬科大学病態生化学研究室・大山　統一郎氏に感謝致します．

文　献

1) 戸川三省，山田剛太郎．高齢者C型慢性肝疾患へのインターフェロン治療．肝胆膵　2002；45：1033—1038
2) Hamada H, Yatsuhashi H, Yano K, et al. Impact of aging on the development of hepatocellular carcinoma in patients with posttransfusion chronic hepatitis C. Cancer 2002; 95 (2): 331—339
3) Yoshida H, Shiratori Y, Moriyama M, et al. Interferon therapy reduces the risk for hepatocellular carcinoma: National surveillance program of cirrhostic and noncirrhotic patients with chronic hepatitis C in Japan. Ann Intern Med 1999; 131: 174—181
4) Yoshizawa H. Trends of hepatitis virus carriers. Hepatol Res 2002; 24: S28—39

5) Nomura H, Tanimoto H, Kajiwara E, et al. Factors contributing to ribavirin-induced anemia. J Gastroen Hepatol 2004; 19: 1312—1317
6) Manns MP, McHutchison JG, Gordon SC, et al. Peginterferon alfa-2b plus ribavirin compared with interferon alfa-2b plus ribavirin for initial treatment of chronic hepatitis C: a randomised trial. Lancet 2001; 358: 958—965
7) Fried MW, Shiffman ML, Reddy KR, et al. Peginterferon alfa-2a plus ribavirin for chronic hepatitis C virus infection. N Engl J Med 2002; 347: 975—982
8) Romero-Gomez M, Del MV, Andrade RJ, et al. Insulin resistance impairs sustained response rate to peginterferon plus ribavirin in chronic hepatitis C patients. Gastroenterology 2005; 128 (3): 636—641
9) D'Souza R, Sabin CA, Foster GR. Insulin resistance plays a significant role in liver fibrosis in chronic hepatitis C and in the response to antiviral therapy. Am J Gastroenterol 2005; 100 (7): 1509—1515
10) Yaginuma R, Ikejima K, Okumura K, et al. Hepatic steatosis is a predictor of poor response to interferon alpha-2b and ribavirin combination therapy in Japanese patients with chronic hepatitis C. Hepatol Res 2006; 35: 19—25
11) Nomura H, Tanimoto H, Kajiwara E, et al. Factors contributing to ribavirin-induced anemia. J Gastroen Hepatol 2004; 19: 1312—1317
12) Hiramatsu N, Oze T, Tsuda N, et al. Should aged patients with chronic hepatitis C be treated with interferon and ribavirin combination therapy? Hepatol Res 2006; 35: 185—189
13) Okanoue T, Sakamoto S, Itoh Y, et al. Side effects of high-dose interferon therapy for chronic hepatitis C. J Hepatol 1996; 25: 283—291
14) Buti M, Mendez C, Schaper M, et al. Hepatitis C virus Core Antigen as a predictor of non-response in genotype 1 chronic hepatitis C patients treated with peginterferon α -2b plus ribavirin. J Hepatol 2004; 40: 527—532
15) Veillon P, Payan C, Pcchio G, et al. Comparative evaluation of the total hepatitis C virus core antigen, branched-DNA, and amplicor monitor assays in determining viremia for patients with chronic hepatitis C during interferon plus ribavirin combination therapy. J Clin Microbiol 2003; 41: 3212—3220
16) Zanetti AR, Romano L, Brunetto M, et al. Total HCV core antigen assay: a new marker of hepatitis C viremia for monitoring the progress of therapy. J Med Virol 2003; 70: 27—30
17) Kim KI, Kim SR, Sasase N, et al. 2′-, 5′-Oligoadenylate synthetase response ratio predicting virological response to PEG-interferon-α 2 b plus ribavirin therapy in patients with chronic hepatitis C. J Clin Pharm Ther 2006; 31: 441—446
18) Yasui K, Okanoue T, Murakami Y, et al. Dynamics of hepatitis C viremia Following interferon-alpha administration. J Infect Dis 1998; 177: 1475—1479
19) Neumann AU, Lam NP, Dahari H, et al. Hepatitis C viral dynamics in vivo and the antiviral efficacy of interferon-alpha therapy. Science 1998; 282: 103—107
20) Anonymous. National Institutes of Health Consensus Development Conference Statement: Management of hepatitis C. Hepatology 2002; 36: S3
21) Anonymous. Consensus conference. Treatment of Hepatitis C. Agence Nationale d'Accreditation et d'Evaluation en Sante (ANAES). Gastroen Clin Biol 2002; 26: B303
22) Schmidt A, Zilberstein A, Shulman L, et al. Interferon action: isolation of nuclease F, a translation inhibitor activated by interferon-induced (2′, 5′) oligoisoadenylate. FEBS Lett 1978; 95: 257
23) Nilsen TW, McCandless S, Baglioni C. 2′, 5′-oligo (A)-activated endonuclease in NIH 3T3 mouse cells chronically infected with Moloney murine leukemia virus. Virology 1982; 122: 498
24) Karino Y, Hige S, Matsushima M, et al. Significance of 2′, 5′-oligoadenylate synthetase activity and HCV genotype in IFN therapy for type C chronic hepatitis. Hokkaido Igaku Zasshi 1994; 69: 1354
25) Toda K, Kumagai N, Iwabuchi N, et al. 2-5AS activity in serum and peripheral blood mononuclear cells for chronic active hepatitis C and the relationship to clinical outcome of interferon therapy. Jpn J Clin Immunol 1997; 20: 428
26) Tong WB, Zhang CY, Feng BF, et al. Establishment of a nonradioactive assay for 2′, 5′ oligoadenylate synthetase and its application in chronic hepatitis C patients receiving interferon-alpha. World J Gastroenterol 1998; 4: 70
27) Yano H, Yanai Y, Momosaki S, et al. Growth inhibi-

tory effects of interferon-α subtypes vary according to human liver cancer cell lines. J Gastroenterol Hepatol 2006; 21: 1720—1725

28) Nomura H, Kashiwagi Y, Hirano R, et al. Efficacy of low dose long-term interferon monotherapy in aged patients with chronic hepatitis C genotype 1 and its relation to alpha-fetoprotein: A Pilot study. Hepatol Res 2007; 37: 490—497

29) Akuta N, Suzuki F, Kawamura Y, et al. Predictors of viral kinetics to peginterferon plus rivavirin combination therapy in Japanese patients infected with hepatitis C virus genotype 1b. J Med Virol 2007; 79 (11): 1686—1695

Pegylated interferon α-2b/ribavirin combination therapy for elderly patients with chronic hepatitis C with high viral load of HCV genotype 1b

Soo Ryang Kim[1]*, Susumu Imoto[1], Shuichi Fuki[1], Ke Ih Kim[2], Miyuki Taniguchi[2], Motoko Nagano[2], Hak Hotta[4], Ikuo Shouji[5], Yoshihiro Kanbara[5], Yoko Maekawa[6], Masatoshi Kudo[7], Yoshitake Hayashi[8]

The patients (n = 75) in this study had chronic hepatitis C with high viral loads of serum HCV-RNA genotype 1b. All the patients received a regimen of pegylated interferon α-2b plus ribavirin (PEG IFN α-2b/RBV) for 48 weeks. Comparative analysis was done by dividing these patients into two groups by age: Elderly group (over 65 years old, 23 patients) and Non-Elderly group (under 65 years old, 52 patients). The sustained viral response (SVR) rate in the Elderly (37.5%, 6/16) was not different significantly from that in the Non-Elderly (50%, 20/40). The response ratio of 2'-5'-oligoadenylate synthetase (2-5AS), the viral dynamics and the rate of discontinuation of therapy were not different between the two groups. Interestingly, however, the mean α-fetoprotein (AFP) values decreased significantly in the Elderly irrespective of SVR or non-SVR (from 10.1 ± 9.55 ng/ml before treatment to 5.18 ± 4.52 ng/ml after treatment, $P<0.05$), but did not in the Non-Elderly. It was thus suggested that Peg IFN α-2b/RBV would be useful in the prevention of HCC in elderly patients including non-SVR cases.

Key words: chronic hepatitis C　pegylated interferon α-2b/ribavirin combination therapy　elderly patients　prevention of hepatocarcinogenesis　AFP

Kanzo 2008; 49: 145—152

1) Department of Gastroenterology, Kobe Asahi Hospital
2) Department of Pharmacy, Kobe Asahi Hospital
3) Medical Information Center, Kobe Asahi Hospital
4) Division of Microbiology, Kobe University Graduate School of Medicine
5) Department of Surgery, Hyogo Cancer Center
6) Department of Surgery, Junshin Hospital
7) Department of Gastroenterology, Kinki University Medical School of Medicine
8) Division of Molecular Medicine & Medical Genetics, Kobe University Graduate School of Medicine
*Corresponding author: asahi-hp@arion.ocn.ne.jp

zjv00509/zjv157709z | xppws | S=1 | 1/6/09 | Art: 1690-08
zjs / DOCHEAD=NOTE zjss / DOCTOPIC=VIRUS-CELL INTERACTIONS
FROM COVER SHEET: Editor: Perlman Article No.: N Section: Interactions

JOURNAL OF VIROLOGY, Mar. 2009, p. 000 Vol. 83, No. 5
0022-538X/09/$08.00+0 doi:10.1128/JVI.01690-08

Proteasomal Turnover of Hepatitis C Virus Core Protein Is Regulated by Two Distinct Mechanisms: a Ubiquitin-Dependent Mechanism and a Ubiquitin-Independent but PA28γ-Dependent Mechanism▽

Ryosuke Suzuki,[1] Kohji Moriishi,[2] Kouichirou Fukuda,[1] Masayuki Shirakura,[1] Koji Ishii,[1] Ikuo Shoji,[3] Takaji Wakita,[1] Tatsuo Miyamura,[1] Yoshiharu Matsuura,[2] and Tetsuro Suzuki[1]*

Department of Virology II, National Institute of Infectious Diseases, Tokyo 162-8640,[1] Department of Molecular Virology, Research Institute for Microbial Diseases, Osaka University, Osaka 565-0871,[2] and Division of Microbiology, Kobe University Graduate School of Medicine, Hyogo 650-0017,[3] Japan

Received 8 August 2008/Accepted 5 December 2008

We have previously reported on the ubiquitylation and degradation of hepatitis C virus core protein. Here we demonstrate that proteasomal degradation of the core protein is mediated by two distinct mechanisms. One leads to polyubiquitylation, in which lysine residues in the N-terminal region are preferential ubiquitylation sites. The other is independent of the presence of ubiquitin. Gain- and loss-of-function analyses using lysineless mutants substantiate the hypothesis that the proteasome activator PA28γ, a binding partner of the core, is involved in the ubiquitin-independent degradation of the core protein. Our results suggest that turnover of this multifunctional viral protein can be tightly controlled via dual ubiquitin-dependent and -independent proteasomal pathways.

Fn1 Hepatitis C virus (HCV) core protein, whose amino acid sequence is highly conserved among different HCV strains, not only is involved in the formation of the HCV virion but also has a number of regulatory functions, including modulation of signaling pathways, cellular and viral gene expression, cell transformation, apoptosis, and lipid metabolism (reviewed in references 9 and 15). We have previously reported that the E6AP E3 ubiquitin (Ub) ligase binds to the core protein and plays an important role in polyubiquitylation and proteasomal degradation of the core protein (22). Another study from our group identified the proteasome activator PA28γ/REG-γ as an HCV core-binding partner, demonstrating degradation of the core protein via a PA28γ-dependent pathway (16, 17). In this work, we further investigated the molecular mechanisms underlying proteasomal degradation of the core protein and found that in addition to regulation by the Ub-mediated pathway, the turnover of the core protein is also regulated by PA28γ in a Ub-independent manner.

Although ubiquitylation of substrates generally requires at least one Lys residue to serve as a Ub acceptor site (5), there is no consensus as to the specificity of the Lys targeted by Ub (4, 8). To determine the sites of Ub conjugation in the core protein, we used site-directed mutagenesis to replace individual Lys residues or clusters of Lys residues with Arg residues in the N-terminal 152 amino acids (aa) of the core (C152), within F1 which is contained all seven Lys residues (Fig. 1A). Plasmids expressing a variety of mutated core proteins were generated by PCR and inserted into the pCAGGS (18). Each core-expressing construct was transfected into human embryonic kidney 293T cells along with the pMT107 (25) encoding a Ub moiety tagged with six His residues (His_6). Transfected cells were treated with the proteasome inhibitor MG132 for 14 h to maximize the level of Ub-conjugated core intermediates by blocking the proteasome pathway and were harvested 48 h posttransfection. His_6-tagged proteins were purified from the extracts by Ni^{2+}-chelation chromatography. Eluted protein and whole lysates of transfected cells before purification were analyzed by Western blotting using anticore antibodies (Fig. 1B). Mutations replacing one or two Lys residues with Arg in the core protein did not affect the efficiency of ubiquitylation: detection of multiple Ub-conjugated core intermediates was observed in the mutant core proteins comparable to the results seen with the wild-type core protein as previously reported (23). In contrast, a substitution of four N-terminal Lys residues (C152K6 to -23R) caused a significant reduction in ubiquitylation (Fig. 1B, lane 9). Multiple Ub-conjugated core intermediates were not detected in the Lys-less mutant (C152KR), in which all seven Lys residues were replaced with Arg (Fig. 1B, lane 11). These results suggest that there is not a particular Lys residue in the core protein to act as the Ub acceptor but that more than one Lys located in its N-terminal region can serve as the preferential ubiquitylation site. In rare cases, Ub is known to be conjugated to the N terminus of proteins; however, these results indicate that this does not occur within the core protein.

To investigate how polyubiquitylation correlates with proteasome degradation of the core protein, we performed kinetic analysis of the wild-type and mutated core proteins by use of the Ub protein reference (UPR) technique, which can compensate for data scatter of sample-to-sample variations such as levels of expression (10, 24). Fusion proteins expressed from UPR-based constructs (Fig. 2A) were cotranslationally cleaved F2 by deubiquitylating enzymes, thereby generating equimolar quantities of the core proteins and the reference protein, dihydrofolate reductase-hemagglutinin (DHFR-HA) tag-modified Ub, in which the Lys at aa 48 was replaced by Arg to prevent its polyubiquitylation (Ub^{R48}). After 24 h of transfec-

* Corresponding author. Mailing address: Department of Virology II, National Institute of Infectious Diseases, 1-23-1 Toyama, Shinjuku-ku, Tokyo 162-8640, Japan. Phone: 81-3-5285-1111. Fax: 81-3-5285-1161. E-mail: tesuzuki@nih.go.jp.

▽ Published ahead of print on 17 December 2008.

zjv00509/zjv157709z | xppws | S=1 | 1/6/09 | Art: 1690-08

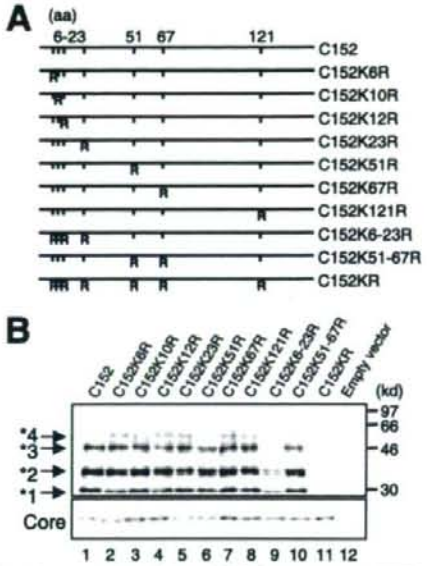

FIG. 1. In vivo ubiquitylation of HCV core protein. (A) The HCV core protein (N-terminal 152 aa) is represented on the top. The positions of the amino acid residues of the core protein are indicated above the bold lines. The positions of the seven Lys residues in the core are marked by vertical ticks. Substitution of Lys with Arg (R) is schematically depicted. (B) Detection of ubiquitylated forms of the core proteins. The transfected cells with core expression plasmids and pMT107 were treated with the proteasome inhibitor MG132 and harvested 48 h after transfection. His_6-tagged proteins were purified and subsequently analyzed by Western blot analysis using anticore antibody (upper panel). Core proteins conjugated to a number of His_6-Ub are denoted with asterisks. Whole lysates of transfected cells before purification were also analyzed (lower panel). Lanes 1 to 11, C152 to C152KR, as indicated for panel A. Lane 12; empty vector.

AQ: A

tion with UPR constructs, cells were treated with cycloheximide and the amounts of core proteins and DHFR-HA-Ub^{R48} at the indicated time points were determined by Western blot analysis using anticore and anti-HA antibodies. The mature form of the core protein, aa 1 to 173 (C173) (13, 20), and C152 were degraded with first-order kinetics (Fig. 2B and D). MG132 completely blocked the degradation of C173 and C152 (Fig. 2B), and C152K6-23R and C152KR were markedly stabilized (Fig. 2C). The half-lives of C173 and C152 were calculated to be 5 to 6 h, whereas those of C152K6-23R and C152KR were calculated to be 22 to 24 h (Fig. 2D), confirming that the Ub plays an important role in regulating degradation of the core protein. Nevertheless, these results also suggest possible involvement of the Ub-independent pathway in the turnover of the core protein, as C152KR is more destabilized than the reference protein (Fig. 2C and 2D).

We have shown that PA28γ specifically binds to the core protein and is involved in its degradation (16, 17). Recent studies demonstrated that PA28γ is responsible for Ub-independent degradation of the steroid receptor coactivator SRC-3 and cell cycle inhibitors such as p21 (3, 11, 12). Thus, we next investigated the possibility of PA28γ involvement in the deg-

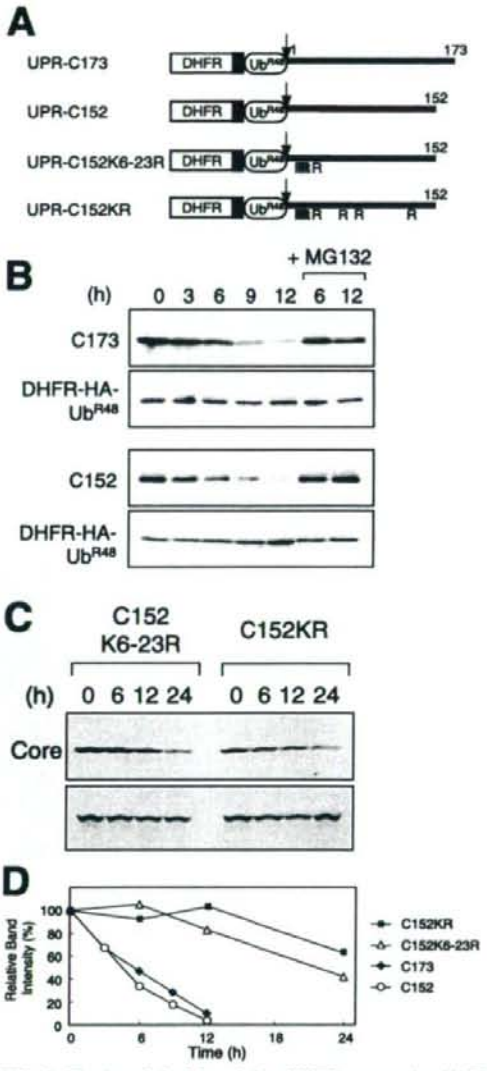

FIG. 2. Kinetic analysis of degradation of HCV core proteins. (A) The fusion constructs used in the UPR technique. Open boxes indicate the DHFR sequence, which is extended at the C terminus by a sequence containing the HA epitope (hatched boxes). Ub^{R48} moieties bearing the Lys-Arg substitution at aa 48 are represented by open ellipses. Bold lines indicate the regions of the core protein. The amino acid positions of the core protein are indicated above the bold lines. The arrows indicate the sites of in vivo cleavage by deubiquitylating enzymes. (B and C) Turnover of the core proteins. After a 24-h transfection with each UPR construct, cells were treated with 50 μg of cycloheximide/ml in the presence or absence of 10 μM MG132 for the different time periods indicated. Cells were lysed at the different time points indicated, followed by evaluation via sodium dodecyl sulfate-polyacrylamide gel electrophoresis and Western blot analysis using antibodies against the core protein and HA. (D) Quantitation of the data shown in panels B and C. At each time point, the ratio of band intensity of the core protein relative to the reference DHFR-HA-Ub^{R48} was determined by densitometry and is plotted as a percentage of the ratio at time zero.

zjv00509/zjv157709z | xppws | S=1 | 1/6/09 | Art: 1690-08

radation of either C152KR or C152. Since C152KR carries two amino acid substitutions in the PA28γ-binding region (aa 44 to 71) (17), we tested the influence of the mutations of C152KR on the interaction with PA28γ by use of a coimmunoprecipitation assay. When Flag-tagged PA28γ (F-PA28γ) was expressed in cells along with C152 or C152KR, F-PA28γ precipitated along with both C152 and C152KR, indicating that PA28γ interacts with both core proteins (Fig. 3A). Figure 3B reveals the effect of exogenous expression of F-PA28γ on the steady-state levels of C152 and C152KR. Consistent with previous data (17), the expression level of C152 was decreased to a nearly undetectable level in the presence of PA28γ (Fig. 3B, lanes 1 and 3). Interestingly, exogenous expression of PA28γ led to a marked reduction in the amount of C152KR expressed (Fig. 3B, lanes 5 and 7). Treatment with MG132 increased the steady-state level of the C152KR in the presence of F-PA28γ as well as the level of C152 (Fig. 3B, lanes 4 and 8).

We further investigated whether PA28γ affects the turnover of Lys-less core protein through time course experiments. C152KR was rapidly destabilized and almost completely degraded in a 3-h chase experiment using cells overexpressing F-PA28γ (Fig. 3C, left panels). A similar result was obtained using an analogous Lys-less mutant of the full-length core protein C191KR (Fig. 3C, right panels), thus demonstrating that the Lys-less core protein undergoes proteasomal degradation in a PA28γ-dependent manner. These results suggest that PA28γ may play a role in accelerating the turnover of the HCV core protein that is independent of ubiquitylation.

Finally, we examined gain- and loss-of-function of PA28γ with respect to degradation of full-length wild-type (C191) and mutated (C191KR) core proteins in human hepatoma Huh-7 cells. As expected, exogenous expression of PA28γ or E6AP caused a decrease in the C191 steady-state levels (Fig. 4A). In contrast, the C191KR level was decreased with expression of PA28γ but not of E6AP. We further used RNA interference to inhibit expression of PA28γ or E6AP. An increase in the abundance of C191KR was observed with PA28γ small interfering RNA (siRNA) but not with E6AP siRNA (Fig. 4B). An increase in the C191 level caused by the activity of siRNA against PA28γ or E6AP was confirmed as well.

Taking these results together, we conclude that turnover of the core protein is regulated by both Ub-dependent and Ub-independent pathways and that PA28γ is possibly involved in Ub-independent proteasomal degradation of the core protein. PA28 is known to specifically bind and activate the 20S proteasome (19). Thus, PA28γ may function by facilitating the delivery of the core protein to the proteasome in a Ub-independent manner.

Accumulating evidence suggests the existence of proteasome-dependent but Ub-independent pathways for protein degradation, and several important molecules, such as p53, p73, Rb, SRC-3, and the hepatitis B virus X protein, have two distinct degradation pathways that function in a Ub-dependent and Ub-independent manner (1, 2, 6, 7, 14, 21, 27). Recently, critical roles for PA28γ in the Ub-independent pathway have been demonstrated; SRC-3 and p21 can be recognized by the 20S proteasome independently of ubiquitylation through their interaction with PA28γ (3, 11, 12). It has also been reported that phosphorylation-dependent ubiquitylation mediated by GSK3 and SCF is important for SRC-3 turnover (26). Never-

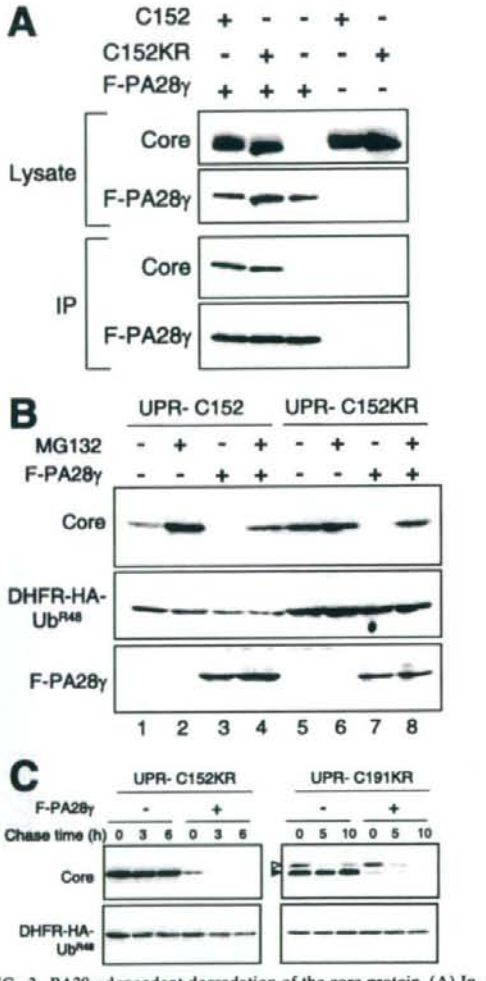

FIG. 3. PA28γ-dependent degradation of the core protein. (A) Interaction of the core protein with PA28γ. Cells were cotransfected with the wild-type (C152) or Lys-less (C152KR) core expression plasmid in the presence of a Flag-PA28γ (F-PA28γ) expression plasmid or an empty vector. The transfected cells were treated with MG132. After 48 h, the cell lysates were immunoprecipitated with anti-Flag antibody and visualized by Western blotting with anticore antibodies. Western blot analysis of whole cell lysates was also performed. (B) Degradation of the wild-type and Lys-less core proteins via the PA28γ-dependent pathway. Cells were transfected with the UPR construct with or without F-PA28γ. In some cases, cells were treated with 10 μM MG132 for 14 h before harvesting. Western blot analysis was performed using anticore, anti-HA, and anti-Flag antibodies. (C) After 24 h of transfection with UPR-C152KR and UPR-C191KR with or without F-PA28γ (an empty vector), cells were treated with 50 μg of cycloheximide/ml for different time periods as indicated (chase time). Western blot analysis was performed using anticore and anti-HA antibodies. The precursor core protein and the core that was processed, presumably by signal peptide peptidase, are denoted by open and closed triangles, respectively.

zjv00509/zjv157709z | xppws | S=1 | 1/6/09 | Art: 1690-08

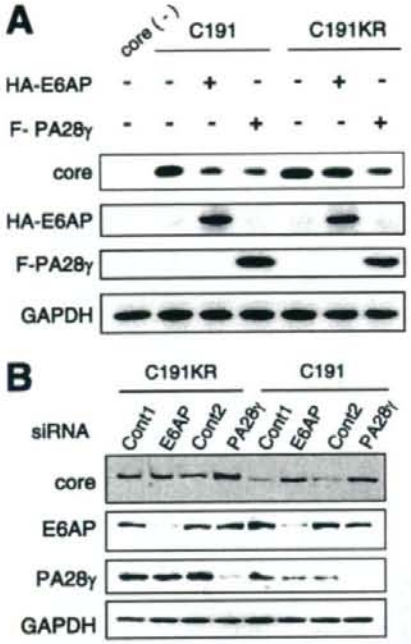

FIG. 4. Ub-dependent and Ub-independent degradation of the full-length core protein in hepatic cells. (A) Huh-7 cells were cotransfected with plasmids for the full-length core protein (C191) or its Lys-less mutant (C191KR) in the presence of F-PA28γ or HA-tagged-E6AP expression plasmid (HA-E6AP). After 48 h, cells were lysed and Western blot analysis was performed using anticore, anti-HA, anti-Flag, or anti-GAPDH. (B) Huh-7 cells were cotransfected with core expression plasmids along with siRNA against PA28γ or E6AP or against negative control siRNA. Cells were harvested 72 h after transfection and subjected to Western blot analysis.

theless, the precise mechanisms underlying turnover of most of the proteasome substrates that are regulated in both Ub-dependent and Ub-independent manners are not well understood. To our knowledge, the HCV core protein is the first viral protein studied that has led to identification of key cellular factors responsible for proteasomal degradation via dual distinct mechanisms. Although the question remains whether there is a physiological significance of the Ub-dependent and Ub-independent degradation of the core protein, it is reasonable to consider that tight control over cellular levels of the core protein, which is multifunctional and essential for viral replication, maturation, and pathogenesis, may play an important role in representing the potential for its functional activity.

This work was supported by a grant-in-aid for Scientific Research from the Japan Society for the Promotion of Science, from the Ministry of Health, Labor and Welfare of Japan, and from the Ministry of Education, Culture, Sports, Science and Technology, by Research on Health Sciences focusing on Drug Innovation from the Japan Health Sciences Foundation, Japan, and by the Program for Promotion of Fundamental Studies in Health Sciences of the National Institute of Biomedical Innovation of Japan.

REFERENCES

1. **Asher, G., J. Lotem, L. Sachs, C. Kahana, and Y. Shaul.** 2002. Mdm-2 and ubiquitin-independent p53 proteasomal degradation regulated by NQO1. Proc. Natl. Acad. Sci. USA **99:**13125–13130.
2. **Asher, G., P. Tsvetkov, C. Kahana, and Y. Shaul.** 2005. A mechanism of ubiquitin-independent proteasomal degradation of the tumor suppressors p53 and p73. Genes Dev. **19:**316–321.
3. **Chen, X., L. F. Barton, Y. Chi, B. E. Clurman, and J. M. Roberts.** 2007. Ubiquitin-independent degradation of cell-cycle inhibitors by the REGγ proteasome. Mol. Cell **26:**843–852.
4. **Ciechanover, A.** 1998. The ubiquitin-proteasome pathway: on protein death and cell life. EMBO J. **17:**7151–7160.
5. **Hershko, A., A. Ciechanover, and A. Varshavsky.** 2000. The ubiquitin system. Nat. Med. **6:**1073–1081.
6. **Jariel-Encontre, I., M. Pariat, F. Martin, S. Carillo, C. Salvat, and M. Piechaczyk.** 1995. Ubiquitinylation is not an absolute requirement for degradation of c-Jun protein by the 26 S proteasome. J. Biol. Chem. **270:**11623–11627.
7. **Jin, Y., H. Lee, S. X. Zeng, M. S. Dai, and H. Lu.** 2003. MDM2 promotes p21waf1/cip1 proteasomal turnover independently of ubiquitylation. EMBO J. **22:**6365–6377.
8. **Ju, D., and Y. Xie.** 2006. Identification of the preferential ubiquitination site and ubiquitin-dependent degradation signal of Rpn4. J. Biol. Chem. **281:**10657–10662.
9. **Lai, M. M. C., and C. F. Ware.** 1999. Hepatitis C virus core protein: possible roles in viral pathogenesis. Springer, Berlin, Germany.
10. **Lévy, F., N. Johnsson, T. Rumenapf, and A. Varshavsky.** 1996. Using ubiquitin to follow the metabolic fate of a protein. Proc. Natl. Acad. Sci. USA **93:**4907–4912.
11. **Li, X., L. Amazit, W. Long, D. M. Lonard, J. J. Monaco, and B. W. O'Malley.** 2007. Ubiquitin- and ATP-independent proteolytic turnover of p21 by the REGγ-proteasome pathway. Mol. Cell **26:**831–842.
12. **Li, X., D. M. Lonard, S. Y. Jung, A. Malovannaya, Q. Feng, J. Qin, S. Y. Tsai, M. J. Tsai, and B. W. O'Malley.** 2006. The SRC-3/AIB1 coactivator is degraded in a ubiquitin- and ATP-independent manner by the REGγ proteasome. Cell **124:**381–392.
13. **Liu, Q., C. Tuckney, R. A. Bhat, A. M. Prince, and P. Zhang.** 1997. Regulated processing of hepatitis C virus core protein is linked to subcellular localization. J. Virol. **71:**657–662.
14. **Lonard, D. M., Z. Nawaz, C. L. Smith, and B. W. O'Malley.** 2000. The 26S proteasome is required for estrogen receptor-α and coactivator turnover and for efficient estrogen receptor-α transactivation. Mol. Cell **5:**939–948.
15. **Moradpour, D., F. Penin, and C. M. Rice.** 2007. Replication of hepatitis C virus. Nat. Rev. Microbiol. **5:**453–463.
16. **Moriishi, K., R. Mochizuki, K. Moriya, H. Miyamoto, Y. Mori, T. Abe, S. Murata, K. Tanaka, T. Miyamura, T. Suzuki, K. Koike, and Y. Matsuura.** 2007. Critical role of PA28γ in hepatitis C virus-associated steatogenesis and hepatocarcinogenesis. Proc. Natl. Acad. Sci. USA **104:**1661–1666.
17. **Moriishi, K., T. Okabayashi, K. Nakai, K. Moriya, K. Koike, S. Murata, T. Chiba, K. Tanaka, R. Suzuki, T. Suzuki, T. Miyamura, and Y. Matsuura.** 2003. Proteasome activator PA28γ-dependent nuclear retention and degradation of hepatitis C virus core protein. J. Virol. **77:**10237–10249.
18. **Niwa, H., K. Yamamura, and J. Miyazaki.** 1991. Efficient selection for high-expression transfectants with a novel eukaryotic vector. Gene **108:**193–199.
19. **Realini, C., C. C. Jensen, Z. Zhang, S. C. Johnston, J. R. Knowlton, C. P. Hill, and M. Rechsteiner.** 1997. Characterization of recombinant REGα, REGβ, and REGγ proteasome activators. J. Biol. Chem. **272:**25483–25492.
20. **Santolini, E., G. Migliaccio, and N. La Monica.** 1994. Biosynthesis and biochemical properties of the hepatitis C virus core protein. J. Virol. **68:**3631–3641.
21. **Sheaff, R. J., J. D. Singer, J. Swanger, M. Smitherman, J. M. Roberts, and B. E. Clurman.** 2000. Proteasomal turnover of p21Cip1 does not require p21Cip1 ubiquitination. Mol. Cell **5:**403–410.
22. **Shirakura, M., K. Murakami, T. Ichimura, R. Suzuki, T. Shimoji, K. Fukuda, K. Abe, S. Sato, M. Fukasawa, Y. Yamakawa, M. Nishijima, K. Moriishi, Y. Matsuura, T. Wakita, T. Suzuki, P. M. Howley, T. Miyamura, and I. Shoji.** 2007. E6AP ubiquitin ligase mediates ubiquitylation and degradation of hepatitis C virus core protein. J. Virol. **81:**1174–1185.
23. **Suzuki, R., K. Tamura, J. Li, K. Ishii, Y. Matsuura, T. Miyamura, and T. Suzuki.** 2001. Ubiquitin-mediated degradation of hepatitis C virus core protein is regulated by processing at its carboxyl terminus. Virology **280:**301–309.
24. **Suzuki, T., and A. Varshavsky.** 1999. Degradation signals in the lysine-asparagine sequence space. EMBO J. **18:**6017–6026.
25. **Treier, M., L. M. Staszewski, and D. Bohmann.** 1994. Ubiquitin-dependent c-Jun degradation in vivo is mediated by the δ domain. Cell **78:**787–798.
26. **Wu, R. C., Q. Feng, D. M. Lonard, and B. W. O'Malley.** 2007. SRC-3 coactivator functional lifetime is regulated by a phospho-dependent ubiquitin time clock. Cell **129:**1125–1140.
27. **Zhang, Z., and R. Zhang.** 2008. Proteasome activator PA28γ regulates p53 by enhancing its MDM2-mediated degradation. EMBO J. **27:**852–864.

Virology 383 (2009) 319–327

Contents lists available at ScienceDirect

Virology

journal homepage: www.elsevier.com/locate/yviro

Cellular vimentin content regulates the protein level of hepatitis C virus core protein and the hepatitis C virus production in cultured cells

Yuko Nitahara-Kasahara [a,1], Masayoshi Fukasawa [a,*], Fumiko Shinkai-Ouchi [a], Shigeko Sato [a], Tetsuro Suzuki [b], Kyoko Murakami [b], Takaji Wakita [b], Kentaro Hanada [a], Tatsuo Miyamura [c], Masahiro Nishijima [a,d]

[a] Department of Biochemistry and Cell Biology, National Institute of Infectious Diseases, 1-23-1, Toyama, Shinjuku-ku, Tokyo 162-8640, Japan
[b] Department of Virology II, National Institute of Infectious Diseases, Tokyo 162-8640, Japan
[c] National Institute of Infectious Diseases, Tokyo 162-8640, Japan
[d] National Institute of Health Sciences, Tokyo 158-8501, Japan

ARTICLE INFO

Article history:
Received 14 August 2008
Returned to author for revision
3 September 2008
Accepted 6 October 2008
Available online 14 November 2008

Keywords:
Hepatitis C virus
Core protein
Vimentin

ABSTRACT

Hepatitis C virus (HCV) core protein is essential for virus particle formation. Using HCV core-expressing and non-expressing Huh7 cell lines, Uc39-6 and Uc321, respectively, we performed comparative proteomic studies of proteins in the 0.5% Triton X-100-insoluble fractions of cells, and found that core-expressing Uc39-6 cells had much lower vimentin content than Uc321 cells. In experiments using vimentin-overexpressing and vimentin-knocked-down cells, we demonstrated that core protein levels were affected by cellular vimentin content. When vimentin expression was knocked-down, there was no difference in mRNA level of core protein; but proteasome-dependent degradation of the core protein was strongly reduced. These findings suggest that the turnover rate of core protein is regulated by cellular vimentin content. HCV production was also affected by cellular vimentin content. Our findings together suggest that modulation of hepatic vimentin expression might enable the control of HCV production.

Introduction

Hepatitis C virus (HCV) is a major causative agent of chronic hepatitis (Choo et al., 1989; Kuo et al., 1989). Persistent HCV infection, which develops in at least 70% of infected patients, is strongly correlated with the development of severe liver diseases such as fibrosis, steatosis, cirrhosis, and hepatocellular carcinomas (HCC). Since more than 170 million people in the world are currently infected with HCV (Choo et al., 1989) and there is no treatment completely effective in curing HCV, HCV infection is one of the most important global public health issues. Understanding of the life cycle of HCV and the mechanism by which HCV induces serious liver diseases is crucial for the development of novel anti-HCV strategies.

HCV is an RNA virus of the *Flaviviridae* family and possesses a single-stranded, positive-sense RNA genome of ~9.6 kb (Bartenschlager and Lohmann, 2000). The HCV RNA genome encodes a polyprotein of ~3000 amino acids that is processed by host and viral proteases into 10 individual components including 4 structural and 6 nonstructural proteins (reviewed by Reed and Rice, 2000). HCV core protein is crucial for virus particle production as the structural component of the viral nucleocapsid and as a unit required for formation of the active HCV replication/assembly complex in host cells (Boulant et al., 2007; Miyanari et al., 2007). In addition, the core protein plays pivotal roles in the pathogenesis of HCV infection, as suggested by the finding that transgenic mice expressing core protein in the liver tend to develop liver steatosis with subsequent HCC (Moriya et al., 1998; Moriya et al., 1997). A large number of studies have revealed that a variety of host proteins interact with the core protein (Suzuki et al., 2007). Although these interactions can markedly affect various biological functions in host cells, it is not clearly known yet which interactions and molecules play roles in HCV production or its pathogenicity. Recent exhaustive gene-silencing analyses of host factors using RNAi demonstrated that RNA helicase DDX3, one of the proteins that interacts with the core, is required for HCV RNA replication as well as HCV production (Ariumi et al., 2007; Randall et al., 2007).

In host hepatic cells, HCV core protein is distributed preferentially in the detergent-resistant fractions (Matto et al., 2004), and HCV RNA replication also occurs on detergent-resistant membranes (Aizaki et al., 2004; Shi et al., 2003), suggesting that host factors in the detergent-resistant fractions play roles in core protein functions. In this study, we focused on HCV core protein and the detergent-insoluble proteins of host cells, and performed comparative targeted proteomic analysis of the detergent-insoluble proteins in HCV core-expressing and non-expressing hepatic cells. We identified vimentin as a protein the amount of which was reduced in core-expressing cell lines, and demonstrated that cellular vimentin content affects levels of HCV core protein through the proteasome-mediated protein

* Corresponding author. Fax: +81 3 5285 1157.
E-mail address: fuka@nih.go.jp (M. Fukasawa).
[1] Present address: National Institute of Neuroscience, National Center of Neurology and Psychiatry, Tokyo 187-8502, Japan.

0042-6822/$ – see front matter © 2008 Published by Elsevier Inc.
doi:10.1016/j.virol.2008.10.009

degradation system. Since cellular vimentin levels ultimately affected HCV production, vimentin may be a novel target for strategies of anti-HCV treatment.

Results

Proteomic analysis of detergent-insoluble fractions (DISFs) by second-dimensional polyacrylamide gel electrophoresis (2D-PAGE)/MALDI-QIT-TOF MS

DISFs and detergent-soluble fractions (DSFs) were prepared from HCV core-expressing Uc39-6 and non-expressing Uc321 cells by a sucrose density gradient ultracentrifugation method as described in Materials and methods. Proteins in the DISFs and DSFs were analyzed by immunoblotting with antibodies to HCV core protein and various organelle markers (Fig. 1A). A significant amount of HCV core protein (~70%) was distributed in the DISF of Uc39-6 cells. Nuclear proteins such as laminA/C and laminB were concentrated only in the DISFs of both types of cells, whereas other organelle proteins such as annexin II (plasma membrane), fatty acid synthase (cytosol), prohibitin (mitochondria), and calnexin (endoplasmic reticulum) were detected in the DSFs but not DISFs (Fig. 1A), suggesting that the DISFs in both types of cells contain minor (~15%) discrete populations of cellular proteins. Next, we performed 2D-PAGE analysis of the DISFs in Uc321 and Uc39-6 cells. Proteins in the DISFs were separated by isoelectric focusing (IEF) (pH 4–7) and 12% sodium dodecyl sulfate (SDS)-PAGE, and visualized by SYPRO-Ruby staining (Fig. 1B). Intensity of each spot in 2-D images was compared between Uc321 and Uc39-6 cells. The most difference in DISF proteins between Uc321 and Uc39-6 cells (the Uc39-6/Uc321 ratios of intensity normalized with actin: 10.8–28.0) was detected in the spots numbered as 1 in Fig. 1B (MW~57 kDa, pI~4.7), in which vimentin alone was identified by mass spectrometric analysis. We therefore focused on the relationship between cellular vimentin and core protein in further investigations.

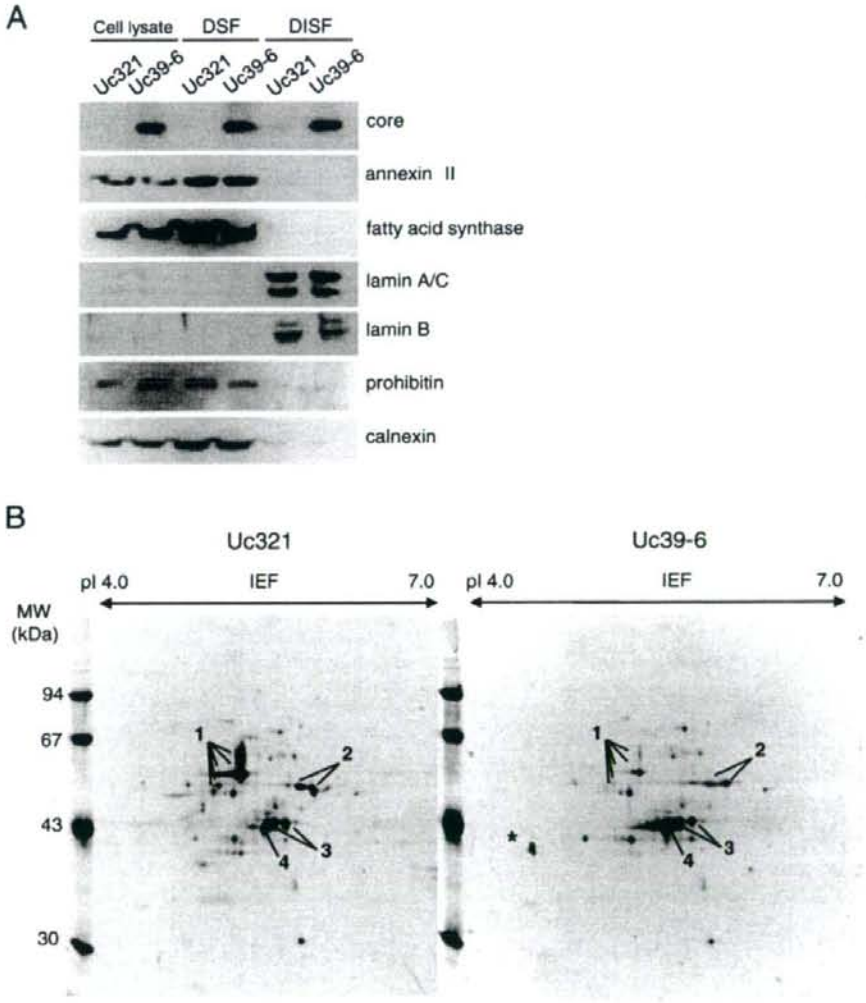

Fig. 1. Immunoblot and 2D-PAGE analysis of DISFs. (A) Total cell lysate fractions (5 μg of protein), DSFs (50 μg of protein), and DISFs (5 μg of protein) from core-expressing Uc39-6 and non-expressing Uc321 cells were analyzed by immunoblotting with antibodies to HCV core protein and various organelle markers as indicated. (B) 2D-PAGE analysis of proteins in DISFs of Uc321 and Uc39-6 cells. Proteins (150 μg) were separated by IEF (pH 4–7), followed by SDS-PAGE on a 12% gel. The gels were stained with SYPRO-Ruby. Major spots, identified as cytoskeletal proteins, are marked: 1, vimentin; 2, cytokeratin 8; 3, cytokeratin 18; 4, actin. *: a non-specific spot.

HCV core-expressing cell lines exhibited reduced vimentin content

To confirm the reduction of vimentin levels in DISFs of HCV core-expressing Uc39-6 cells, immunoblot analysis was performed using anti-vimentin antibody. Uc39-6 cells exhibited lower vimentin contents not only in DISF but also the total cell lysate fraction compared with control Uc321 cells (Fig. 2A). Similar results were obtained in the cell lysate fraction of another independent clone of an HCV core-expressing Huh7 cell line, Uc39-2 (Fig. 2B). Furthermore, a core-expressing hepatic HepG2 cell line, Hep39, also had lower vimentin content than a control cell line, Hepswx (Fig. 2C). These findings exclude the possibility that the reduction of vimentin levels in core-expressing cell lines is a clone- or cell-specific event. Consistent with these findings, levels of vimentin mRNA in Uc39-2 and Uc39-6 cells were also lower than that in Uc321 cells (data not shown). Taken together, these findings demonstrate marked reduction of vimentin expression in HCV core-expressing cell lines.

Cellular vimentin content affects the protein level of HCV core protein

To investigate the relationship between HCV core protein and vimentin, we examined the effect of cellular vimentin content on level of HCV core protein. When the expression of vimentin or control hypoxanthine guanine phosphoribosyltransferase 1 (HPRT) was knocked down in Uc39-6 cells by siRNA treatment, the protein level of HCV core protein in vimentin-knocked-down cells was significantly higher than those in siRNA-untreated and HPRT-knocked-down cells (Fig. 3A). On the other hand, cellular mRNA levels of HCV core protein, corrected for β-actin mRNA content, did not differ substantially among these types of cells (Table 1). These findings revealed that post-translational steps were involved in the increase of HCV core protein level in vimentin-knocked-down cells. Next, we established a vimentin-overexpressing Huh7 cell line, Huh7/vimentin, and compared the level of the core protein in Huh7/vimentin cells with that in control Huh7/hygro cells after transient expression of the core protein with pcEF39neo vector. After 9-day culture with G418 selection, the viabilities of the two types of cells were similar, though the level of expression of the core protein in Huh7/vimentin was significantly lower than that in Huh7/hygro cells (Fig. 3B). These findings demonstrated that level of HCV core protein was inversely correlated with cellular vimentin content, and thus strongly suggested that it was affected by cellular vimentin content.

We further attempted to verify these effects of vimentin using the vimentin-null cell line 1HF5 and the vimentin-expressing control cell line 2CB5, derived from human adrenal carcinoma SW13 cells (Sarria et al., 1990). When 1HF5 and 2CB5 cells were transfected with the core expression vector pcEF39neo and cultured with G418 selection, the viabilities of the two types of cells were similar, though the level of expression of the core protein in 1HF5 cells was much higher than that in 2CB5 cells (Fig. 3C), consistent with the results in Figs. 3A, B. An exogenously vimentin-expressing 1HF5 cell line carrying pcDNA3.1/Hygro/vimentin, 1HF5/vimentin, and a control vimentin-null cell line carrying pcDNA3.1/Hygro, 1HF5/hygro, were then established, and transfected with the green fluorescent protein (GFP)-expressing pcDNA3.1/EGFP vector, the core-coding pcEF39neo vector, or the control pcFE321swxneo vector. After selection under G418 for 9 days, the viabilities of these transfected cells were nearly the same. The levels of expression of GFP were similar in 1HF5/hygro and 1HF5/vimentin cells, while the core protein level in 1HF5/vimentin cells was significantly lower than that in 1HF5/hygro cells (Fig. 3D), consistent with the results in Fig. 3B.

These findings together indicate that cellular vimentin content regulates the level of HCV core protein in post-translational fashion.

Vimentin is involved in proteasomal degradation of core proteins in cells

HCV core proteins are known to be preferentially degraded by the proteasome-dependent pathway (Suzuki et al., 2001). To determine whether cellular vimentin content affects proteasome-dependent degradation of the core protein, we examined the effects of the proteasome inhibitor MG132 on core protein levels in vimentin-knocked-down cells. After Huh7 cells transfected with pCAG/Flag-core (Huh7/Flag-core cells) had been treated with MG132 for 16 h, cellular accumulation of core protein was analyzed by immunoblot (Fig. 4; lanes 3 vs 4), which indicated substantial proteasomal degradation of the core proteins in cultured cells, as described previously (Hope and McLauchlan, 2000; McLauchlan et al., 2002; Suzuki et al., 2001). Huh7/Flag-core cells transfected with control and HPRT siRNA duplexes exhibited similar increases in core protein levels by treatment with MG132 (Fig. 4; lanes 5 vs 6, and 9 vs 10). On the other hand, vimentin-knocked-down Huh7/Flag-core cells that were transfected with vimentin siRNA duplexes exhibited higher content of core protein (lane 7) than the other siRNA-treated cells (lanes 5 and 9), and MG132 treatment resulted in no significant difference in core protein levels in vimentin-knocked-down cells (lanes 7 and 8), indicating that proteasomal degradation of core proteins was markedly inhibited in the vimentin-knocked-down cells. These observations strongly suggested that vimentin plays an important role in the proteasome-mediated proteolytic pathway of the HCV core protein.

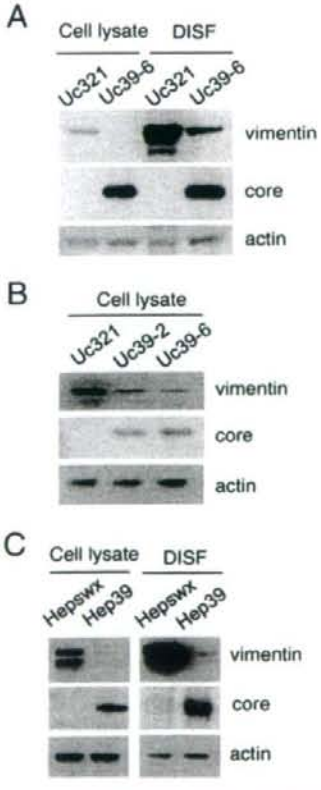

Fig. 2. Immunoblot analysis of vimentin in HCV core-expressing cell lines. Cell lysate fractions and DISFs from various cell lines were analyzed by immunoblotting with antibodies to vimentin, HCV core protein, and β-actin as indicated: cell lysate fractions and DISFs from Uc321 and Uc39-6 cells in (A), cell lysate fractions from Uc321, Uc39-2, and Uc39-6 cells in (B), and cell lysate fractions and DISFs from Hepswx and Hep39 cells in (C). Amounts of protein loaded were 18 μg in (A) and (B), and 5 μg in (C).

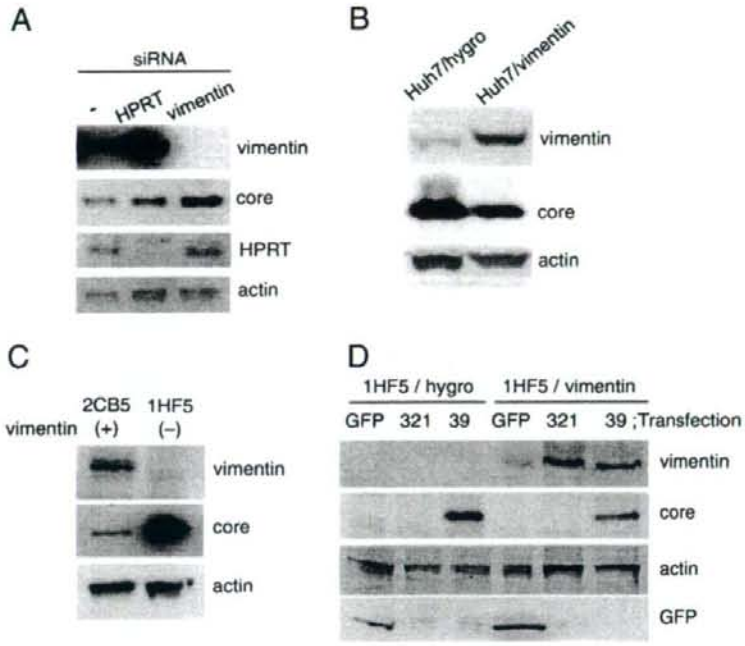

Fig. 3. Effects of cellular vimentin content on the level of expression of HCV core protein. Cellular level of expression of vimentin, HCV core protein, HPRT, β-actin, and GFP were analyzed by immunoblotting of total cell lysates (40 μg of protein) from various cells using specific antibodies. (A) Uc39-6 cells were transfected twice with a 2-day interval without (-) or with vimentin or control HPRT siRNA duplexes. Four days after the first transfection, cell lysates were collected and analyzed. (B) Huh7/hygro and Huh7/vimentin cells were transfected with the core protein-expression vector pcEF39neo, and selected under 1 mg/ml of G418 for 9 days. (C) The 2CB5 (vimentin+) and 1HF5 (vimentin−) lines of SW13 cells were transfected with pcEF39neo, and selected under 1 mg/ml of G418 for a week, followed by additional 2-week culture in normal culture medium. (D) 1HF5/hygro and 1HF5/vimentin cells were transfected with pcDNA3.1/EGFP (GFP), pcFE321swxneo (321), or pcEF39neo (39), and selected under 1 mg/ml of G418 for 9 days.

Under the various siRNA-treated conditions in Fig. 4, we also examined the protein levels of p53, one of the endogeneous host proteins the degradation of which is mainly regulated by proteasomal system (Morimoto et al., 2008). The pattern of p53 protein levels was very similar to that of core protein levels (Fig. 4), suggesting that the vimentin-dependent proteasomal degradation is not specific for the viral core protein. Vimentin-dependent proteasomal degradation system might be generally important for the turnover of endogeneous cellular proteins as well as the viral core protein.

Cellular vimentin contents affect HCV production

Since the level of expression of HCV core protein was affected by cellular vimentin content, we examined whether HCV production was also affected by cellular vimentin content. Infectious HCV (JFH1 strain) particles were used for the following infection assays. HCV production activity was determined by quantification of HCV core protein levels in the infected cells and culture supernatants. We first tested the effect of vimentin knockdown on HCV production. Examination of HCV-infected Huh7 cells treated with vimentin siRNA revealed higher amounts of HCV core protein in both cells and culture medium than examination of non-treated and control HPRT siRNA-treated cells (Fig. 5A). To examine whether the core protein levels in the cell-cultured media reflect the content of infectious HCV particles in them, Huh7 cells were treated with cell-cultured medium containing equal amounts (1.4 fmol) of the core protein collected from each type of cell described in Fig. 5A, and cellular levels of production of the core protein were determined by immunoblot analysis. They were nearly the same among the cells treated with each culture medium (Fig. 5B). These findings indicated that reduction of vimentin expression in Huh7 cells leads to more active HCV production and enhanced release to the supernatant.

We next examined the effects of vimentin overexpression on HCV production. When vimentin-overexpressing Huh7/vimentin and control Huh7/hygro cells were infected with HCV particles, Huh7/vimentin cells exhibited lower amounts of intracellular and extracellular HCV core protein than Huh7/hygro cells (Fig. 5C). Consistent with the results in Fig. 5A, these findings suggested that higher expression of vimentin in host cells resulted in lower HCV production.

We also examined the effect of vimentin knockdown on HCV RNA replication using a JFH1-subgenomic replicon (Fig. 5D). There were no significant differences in replication activities between vimentin-knocked-down cells and the other control cells. These findings indicated that cellular level of vimentin has no effects on HCV non-structural proteins which serve as a unit of RNA replication machinery of HCV. Collectively, these results demonstrated that HCV production activity but not HCV-RNA replication was inversely correlated with cellular vimentin content.

Table 1
mRNA levels of HCV core protein and β-actin in vimentin-knocked-down Uc39-6 cells

	siRNA		
	-	HPRT	vimentin
HCV core ($\times 10^4$ copies/μg total RNA)	2.9±0.3	1.7±0.1	3.0±0.2
β-actin ($\times 10^7$ copies/μg total RNA)	3.0±0.1	1.4±0.1	2.3±0.0
HCV core/β-actin[a]	1	1.3	1.3

Total RNA was isolated from Uc39-6 cells that had been treated twice with a 2-day interval with HPRT siRNA duplexes, with vimentin siRNA duplexes or without (-) either of them, and cultured for 4 days. mRNA levels of HCV core protein and β-actin (a control housekeeping gene) were determined by quantitative real-time PCR. Values are the mean±SD for three determinations.

[a] Numbers represent the relative amounts of HCV core protein mRNA normalized to β-actin level.

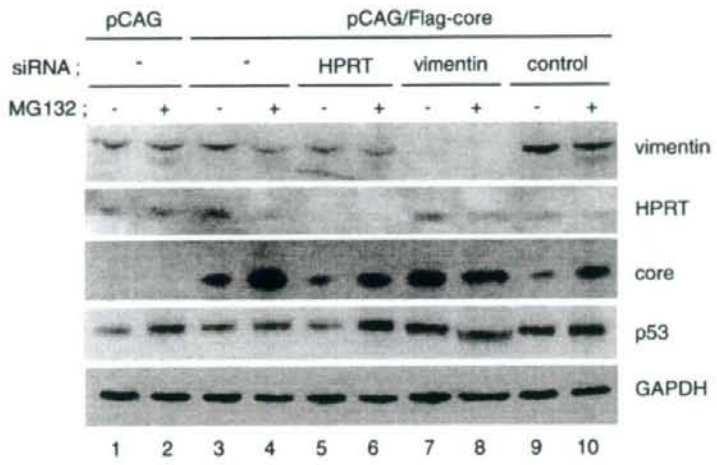

Fig. 4. Effects of the proteasome inhibitor MG132 on level of expression of HCV core protein in Huh7 cells. siRNA duplexes of control, HPRT, or vimentin, together with the core protein-expression vector pCAG/Flag-core, were transfected into Huh7 cells. After 2 days, transfection of these siRNAs was repeated. Cells were further cultured for 2 days and treated with (+) or without (−) MG132 (50 μM) for 16 h. Equivalent amounts of cell lysates were analyzed by immunoblotting with antibodies to vimentin, HPRT, core protein, p53, and GAPDH.

Furthermore, expression of vimentin and HCV core protein in Huh7 cells after HCV infection was observed by immunofluorescence microscopy (Fig. 5E), and the fluorescent intensity of vimentin in core-positive and core-negative Huh7 cells under HCV-infected conditions was determined (Fig. 5F). HCV-infected cells stained with the core-specific antibody always had lower vimentin content (Figs. 5E, F). Moreover, as shown in Fig. 5F, HCV core-negative cells exhibited more variable vimentin levels, whereas the core-positive cells had vimentin levels within a narrow range. These observations, which showed that a Huh7 cell population with lower vimentin content can preferentially produce HCV, were consistent with the results shown in Figs. 5A, C.

Finally, we examined the effects of MG132 on HCV core protein levels in HCV-infected cells in which vimentin was knocked-down or overexpressed. In the presence of MG132, non-treated and control HPRT siRNA-treated cells showed the significant increase of cellular HCV core protein levels, whereas vimentin-knocked-down cells did not (Fig. 5G). These results were consistent with those using HCV core-expressing cells (Fig. 4). HCV core content in vimentin-overexpressing Huh7/vimentin cells was lower than that in control Huh7/hygro cells, but after MG132 treatment Huh7/vimentin and Huh7/hygro cells showed the similar HCV core protein levels (Fig. 5H). Taken together, these results demonstrated the significant involvement of vimentin in proteasome-dependent degradation of HCV core protein in HCV-infected cells (Figs. 5G, H), as well as in HCV core-expressing cells (Fig. 4).

Discussion

By comparative proteomic analysis of the detergent-insoluble proteins in HCV core-expressing and non-expressing Huh7 cell lines, vimentin, an intermediate filament protein, was identified as the protein with the most dramatic reduction in level in the detergent-insoluble fraction of HCV core-expressing Uc39-6 cells (Figs. 1B and 2). On the other hand, there were no significant differences in the amounts of other major proteins including cytoskeletal components such as actin and cytokeratin 8/18 in the detergent-insoluble fractions between the core-expressing and non-expressing cells (Fig. 1B). These findings, together with similar results for other core-expressing cells (Fig. 2), suggested the existence of a specific relationship between the core protein and cellular vimentin. Consistent with these findings, immunofluorescence microscopic analysis of core-expressing cells (data not shown) and HCV-infected cells (Figs. 5E, F) showed that cells with intrinsic lower amount of vimentin are more permissive for higher HCV core protein content.

Knockdown of vimentin expression by siRNA treatment resulted in an increase in HCV core protein levels (Fig. 3A), while overexpression of vimentin reduced core protein contents (Fig. 3B). Similar results were obtained in the experiments using the vimentin-null cell line 1HF5 derived from SW13 cells (Figs. 3C and D). On the other hand, transient knockdown and overexpression of the core proteins in Uc39-6 and Huh7 cells, respectively, did not result in differences in cellular vimentin content (data not shown). These findings indicated that cellular vimentin level affects the level of expression of the core protein but not vice versa. Although transient expression of the core protein did not affect cellular vimentin content, why do various stable cell lines expressing the core protein have lower vimentin level? Since it was very hard to establish the cells stably expressing the core protein, we speculate that only the minor cell population innately having lower vimentin content was able to maintain the substantial core expression levels and was therefore selected.

We next demonstrated that vimentin affects core protein levels in post-translational fashion (Table 1) and is required for the proteasomal degradation of core protein in core-expressing cells (Fig. 4) and also in HCV-infected cells (Figs. 5G, H). Many studies with proteasome inhibitors have shown that a major pathway of degradation of core protein is mediated by the proteasomal system (Hope and McLauchlan, 2000; McLauchlan et al., 2002; Moriishi et al., 2003; Suzuki et al., 2001). PA28γ, a REG family proteasome activator also known as REGγ and Ki antigen, which is located in the nucleus, was shown to play an important role in the proteasomal degradation of the core protein (Moriishi et al., 2003). It was recently reported that the ubiquitin ligase E6AP, which is distributed in the perinuclear cytoplasm and colocalized with the core protein, is also involved in ubiquitylation and degradation of core protein (Shirakura et al., 2007). Vimentin filaments extend from the nuclear membrane toward the cell periphery. In addition, vimentin is known to colocalize with ubiquitinated protein aggregates and form aggresomes when the capacity of the proteasome is exceeded (Johnston et al., 1998). Pull-down assays against the core protein in core-expressing Huh7 cells indicated that a minor portion of cellular vimentin can interact with HCV core protein (data not shown), as

Kang et al. had reported previously (Kang et al., 2005). Co-staining of cellular vimentin and the core protein on immunofluorescence microscopy also supported the existence of a minor but definite association between them (data not shown). Based on these findings, we speculate that vimentin plays a role in the transport of the core protein to the nucleus, where it is then degraded, although further biochemical studies will be needed to demonstrate this.

HCV core protein is distributed mainly in the ER and lipid droplets in host cells (Barba et al., 1997), and the ER membrane associating the lipid droplets with core protein has been recognized as a site important for HCV production, particularly HCV RNA replication and virus particle assembly (Boulant et al., 2007; Miyanari et al., 2007). Vimentin is also closely associated with lipid droplets (Brasaemle et al., 2004; Lieber and Evans, 1996; Schweitzer and Evans, 1998). Thus, in addition to its degradative modulation of core protein, vimentin might also affect the function of lipid droplets and consequently inhibit HCV production. The effects of vimentin knock-down and overexpression on HCV production were actually stronger at the extracellular core protein level (secretion

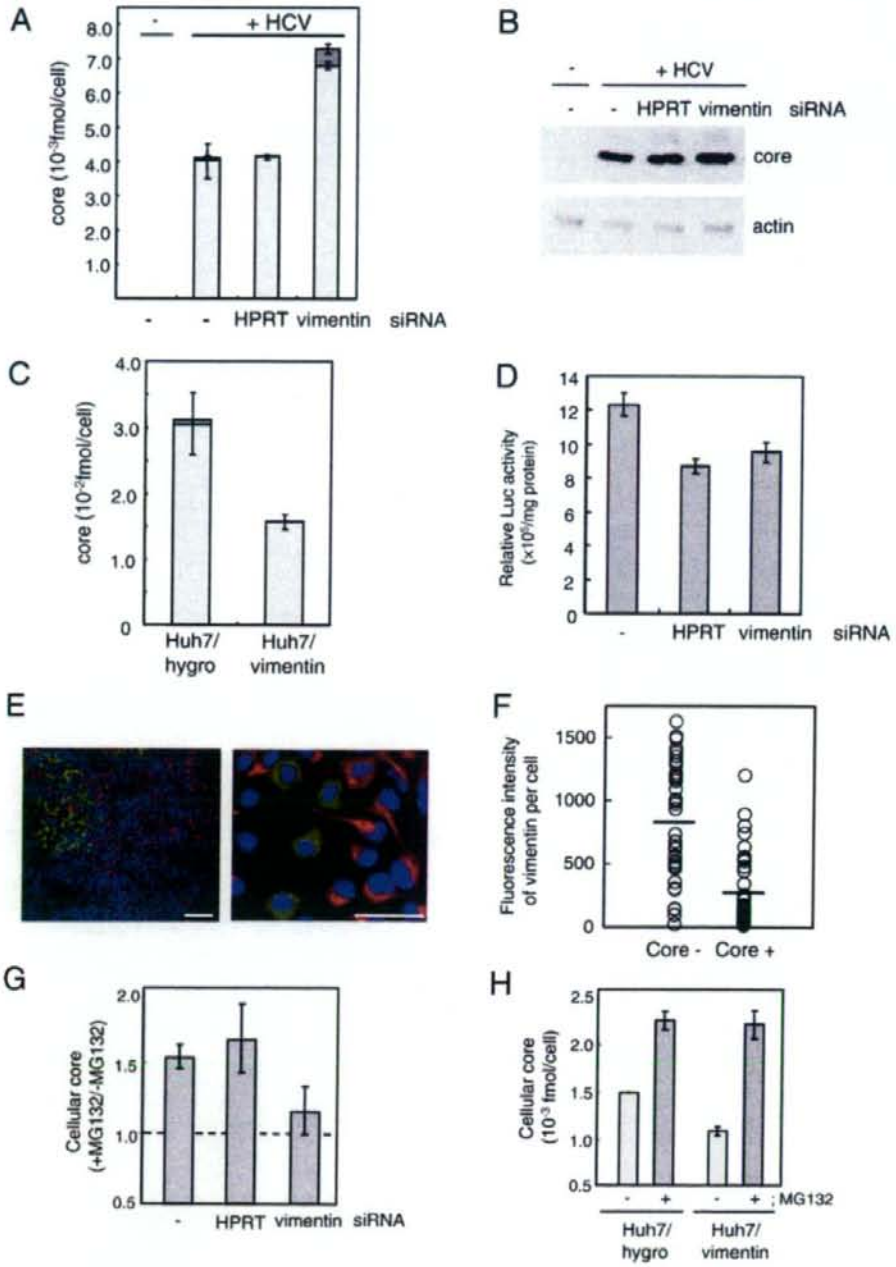

of the virus) than at the intracellular core protein level (Figs. 5A, C), suggesting additional activity of vimentin in the processes of HCV particle release.

Since the level of expression of vimentin in carcinomas is correlated with parameters of malignant potential such as tumor grade and tumor invasion, vimentin has been used as a marker of malignant tumors (Bannasch et al., 1982). It has indeed been reported that some HCV-infected patients with hepatocellular carcinoma exhibited up-regulation of vimentin expression in tumor tissue (Kim et al., 2003) although further statistical studies are required to clearly demonstrate this. Tanaka et al. noted that in livers of HCV-infected patients with hepatocelllular carcinoma the virus existed predominantly in non-cancerous tissue, at levels 10- to 100-fold higher than in cancerous tissue (Tanaka et al., 2004). These observations in human liver samples suggest that the reduction in HCV levels in hepatic tumor can be explained by the increase of vimentin expression in tumor, consistent with our findings for cultured cells.

In this study we demonstrated that cellular vimentin expression enhanced the proteasomal degradation of core protein and eventually restricted HCV production. Vimentin itself and sites of vimentin/core interaction may thus be novel targets of treatment using anti-HCV strategies.

Materials and methods

Antibodies

Mouse monoclonal antibodies to annexin II, fatty acid synthase, calnexin, lamin A/C, and GFP were purchased from BD Transduction Laboratories. Mouse monoclonal antibodies to HCV core protein, prohibitin, and glyceraldehyde-3-phosphate dehydrogenase (GAPDH) were from Anogen, Lab Vision, and Abcam, respectively. Rabbit polyclonal antibodies to vimentin, lamin B1, p53, and HPRT were from Santa Cruz Biotechnology Inc., while those to actin were from Biomedical Technologies Inc.

Plasmids

The mammalian expression vector of HCV core protein, pcEF39neo (Ruggieri et al., 1997), and the empty vector pcEF321swxneo (Harada et al., 1995) were described previously. The mammalian expression vector of Flag-tagged HCV core protein, pCAG/Flag-core, and the empty vector, pCAG, were described previously (Moriishi et al., 2003). For construction of a mammalian expression vector of vimentin, pcDNA3.1/Hygro/vimentin, vimentin fragment was amplified by PCR using the reverse-transcribed cDNAs of Huh7 cells as a template. The PCR primer pairs used were 5′-GCCATGTCCACCAGGTCCGTGTCC-3′ and 5′-TTATTATTCAAGGTCATCGTGATG-3′. The PCR products were inserted into the EcoRV site of pBluescript SKII(+). pBluescript SK(+)/vimentin was digested with Hind III and Xba I, and the vimentin fragment was inserted into pcDNA3.1/Hygro (Invitrogen), which had been digested with Hind III and Xba I. For construction of pcDNA3.1/EGFP, EGFP fragment was prepared by digestion of pEGFP-N1 (Clontech Laboratories, Inc.) with Nhe I and Hind III and inserted into pcDNA3.1/Hygro, which had been digested with Nhe I and Hind III. The subgenomic replicon constructs, pSGR-JFH1/Luc (wild type) and pSGR-JFH1/Luc-GND (GND mutation in the NS5B sequence), with the firefly luciferase reporter gene were described previously (Kato et al., 2005).

Cell lines

All hepatic cells used in this study were plated on collagen-coated dishes (Asahi Techno Glass, Japan). Human hepatic Huh7 and Huh7.5.1 cells were grown in normal culture medium [Dulbecco's modified Eagle's medium (DMEM) (KOJIN BIO, Japan) supplemented with 10% fetal bovine serum (FBS), 100 U/ml Penicillin G, and 100 mg/ml streptomycin sulfate] containing 0.1 mM non-essential amino acids (GIBCO) under a 5% CO_2 atmosphere at 37 °C. We used human hepatic cell lines constitutively expressing HCV core protein, including Hep39 from HepG2 cells (Harada et al., 1995; Ruggieri et al., 1997) and Uc39-2 and Uc39-6 from Huh7 cells (Fukasawa et al., 2006; Sato et al., 2006). Huh7 and HepG2 cell lines carrying the empty vector, Hepswx and Uc321, respectively, were used as a mock control. All of these stable transfectants were maintained in normal culture medium containing 1 mg/ml G418 (Sigma). The human adrenal carcinoma cell line SW13, the subtypes 2CB5 and 1HF5 of which do or do not express vimentin, respectively (Sarria et al., 1990), was maintained in normal culture medium. When the pcDNA3.1/EGFP vector was transfected into 2CB5 and 1HF5 cells, the percentage of GFP-positive cells was 56.3% and 53.6%, respectively, 2 days after transfection ($n=3$), indicating that there was no difference in the transfection efficiency between these cells. To establish vimentin-overexpressing cells, pcDNA3.1/Hygro/vimentin was transfected into 1HF5 and Huh7 cells using FuGENE 6 transfection regent (Roche). The vimentin-overexpressing Huh7 and 1HF5 cells were selected under hygromycin for 2 weeks and cloned to obtain Huh7/vimentin cells and 1HF5/vimentin cells, respectively. Huh7 and 1HF5 cells carrying the empty vector pcDNA/Hygro were also established, as Huh7/hygro cells and 1HF5/hygro cells, respectively.

Preparation of DISFs

Confluent monolayers of Uc321 and Uc39 cells in four culture dishes (150 mm inner diameter) were harvested by trypsinization, and 1.5×10^7 cells of each were pelleted by centrifugation (218 ×g for 5 min at 4 °C). After washing with PBS three times, each cell pellet was resuspended in 1 ml of lysis buffer [10 mM HEPES-HCl, pH 7.5, 10 mM NaCl, 140 mM KCl, 0.5 mM DTT, 0.5% Triton X-100 (Pierce Biotechnology), 10 mM NaF, Complete™ EDTA-free (Roche)] (i.e. a 20% cell suspension). The cell suspension was lysed with a ball-bearing homogenizer (Hope et al., 2002). The soluble fraction (designated the detergent-soluble fraction, DSF) containing ~85% of the total cellular proteins was collected by centrifugation of the cell

Fig. 5. HCV production in vimentin-knockdown and vimentin-overexpressing Huh7 cells. (A) Huh7 cells (5×10^4 cells) in 48-well plates were incubated with or without HCV particles (including 8.0 fmol of core protein) for 6 h, and then treated twice with a 3-day interval without (−) or with siRNA duplexes of HPRT or vimentin. After 7-day culture, the amounts of HCV core protein per cell in cells (light gray bar) and culture medium (dark gray bar) were determined. $n=3$. (B) Culture medium was collected at day 6 in the infection experiment described above in (A). The concentration of HCV core protein in these samples of medium was adjusted to 2.7 fmol/ml with fresh medium. Cells were infected with these samples of medium containing 1.4 fmol of HCV core protein for 2 days, and harvested after 7-day incubation. Infectivity was analyzed by the immunoblotting of cell lysates with antibodies to HCV core protein and β-actin. (C) Vimentin-overexpressing Huh7/vimentin and control Huh7/hygro cells infected with HCV were harvested after 7-day incubation. The amounts of HCV core protein per cell in cells (light gray bar) and culture medium (dark gray bar) were determined. (D) Huh7 cells harboring the HCV subgenomic replicon containing a luciferase reporter gene were transfected without (−) or with siRNA duplexes of HPRT or vimentin. After 2.5-day culture, luciferase activity in cell extracts was determined. $n=3$. (E) Immunofluorescence microscopic analysis of HCV-infected Huh7 cells. After infection with HCV, Huh7 cells were cultured for 6 days. HCV core protein (green) and vimentin (red) were then detected with specific antibodies. Nuclei (blue) were stained with DAPI. Two views showing low and high magnifications are displayed. Bars, 100 μm in the left panel; 50 μm in the right panel. (F) Under the HCV-infected conditions in panel E, fluorescence intensity of vimentin in core-positive and core-negative Huh7 cells was determined by line profile analysis. $n=40$. Statistical significance of differences in fluorescence intensity of vimentin between core-positive and core-negative cells was evaluated using Student's t test, showing $p<10^{-8}$. (G) As in (A), Huh7 cells were incubated with HCV particles, and then treated twice with a 2-day interval without (−) or with siRNA duplexes of HPRT or vimentin. After 4.5-day culture, cells were treated with (+) or without (−) MG132 (50 μM) for 16 h. In each culture condition, the ratio of HCV core protein level in the MG132-treated cells to that in MG132-untreated cells was determined. $n=3$. (H) Huh7/vimentin and Huh7/hygro cells infected with HCV were cultured for 4 days and treated with (+) or without (−) MG132 (50 μM) for 16 h. The amounts of cellular core protein per cell were determined. $n=3$.

lysate performed twice at 218 ×g for 5 min at 4 °C. The insoluble pellet was suspended in 2 ml of lysis buffer containing 1.62 M sucrose and then centrifuged at 10,000 ×g for 1 h at 4 °C. The pellet was resuspended in 1 ml of lysis buffer containing 1.0 M sucrose and layered over 2 ml of lysis buffer containing 2.0 M sucrose. After centrifugation at 50,000 ×g for 2 h at 4 °C, the precipitated fraction containing ~15% of total cellular proteins was collected and resuspended in lysis buffer containing 0.25 M sucrose at a concentration of 3 mg protein/ml (designated the detergent-insoluble fraction, DISF). Each fraction was stored at −80 °C until use. The protein concentrations in these preparations were determined with BCA protein assay reagents (Pierce Biotechnology) using BSA as a standard.

2D-PAGE/MALDI-QJT-TOF MS analysis

The DISF (0.15 mg protein) of each cell line was cleaned using a PlusOne™ 2-D Clean Up kit (GE Healthcare) and resuspended in rehydration solution containing 9 M urea, 4% CHAPS, 65 mM dithioerythritol, and 0.5% ampholyte. The first-dimensional IEF was performed with an Immobiline Dry Strip pH 4–7 according to the manufacturer's instruction (GE Healthcare). The second-dimensional electrophoresis was carried out on 12% SDS-polyacrylamide gel, and the gel was stained with SYPRO-Ruby (Bio-Rad). Spot detection and comparison in 2D images were accomplished with PDQuest™ 2-D analysis software ver. 7.3 (Bio-Rad). The protein bands were excised from the gel and subjected to in-gel trypsin digestion. The tryptic peptide mixtures were analyzed by MALDI-QJT-TOF MS (AXIMA-QJT, Shimazu Biotech, Japan) as described previously (Sato et al., 2006; Shevchenko et al., 1996). Mascot software (Matrix Science) was used for protein identification.

Immunoblot analysis

The proteins were separated by electrophoresis in precast NuPAGE 10% or 12% Bis–Tris gels (Invitrogen), and then transferred to a polyvinylidene difluoride membrane. The membranes were blocked overnight at 4 °C or for 60 min at room temperature in Tris-buffered saline containing 0.1% Tween 20 and 5% skim milk. The blots were probed with the first antibodies at 1:1000 dilution for 60 min at room temperature and then incubated with horseradish peroxidase (HRP)-conjugated goat anti-rabbit IgG (Bio-Rad) or HRP-conjugated goat anti-mouse IgG (GE Healthcare) at 1:2000 dilution for 45 min. Detection of immunoreactive proteins was performed using an ECL system (GE Healthcare).

Quantitative real-time PCR analysis

Cellular total RNAs were prepared with an RNeasy kit (Qiagen). The total RNA fraction (1 μg) was processed directly to cDNA using a Transcriptor First Strand cDNA Synthesis Kit (Roche). Of the total 20 μl cDNA solution, an aliquot of 0.5–2 μl was used for each real-time PCR assay. The PCR primers used for HCV core protein were: forward, 5′-AGGAAGACTTCCGAGCG-3′, and reverse, 5′-GGGTGACAGGAGCCATC-3′. The PCR primers for actin were obtained from the LightCycler™-Primer Set (Roche). Quantitative real-time PCR was carried out in a LightCycler (Roche) using LightCycler-FastStart DNA Master SYBR Green I (Roche).

Transfection of siRNA

Subconfluent cells cultured in a 48-well plate were transfected twice at a 2- or 3-day interval with 30 nM of vimentin-specific, HPRT-specific, or negative control (Invitrogen) siRNA duplexes using Lipofectamine RNAiMAX (Invitrogen) following the manufacturer's instructions. The siRNA target sequences were as follows: vimentin (sense), 5′-ACCTTGAACGCAAAGTGGAATCTTT-3′; HPRT-S1 (sense), 5′-AAGCCAGACUUUGUUGGAUUUGAAA-3′.

Infection of Huh7 cells with HCV

Infectious HCV (JFH1 strain) particles were produced in Huh7.5.1 cells as described previously (Wakita et al., 2005). Culture supernatant containing infectious HCV particles was collected and stored at −80 °C until use. Subconfluent naïve Huh7, Huh7/hygro, or Huh7/vimentin cells in 24-well or 48-well plates were exposed to normal culture medium containing HCV particles (1.4–8 fmol core protein/well, corresponding to moi=0.0175–0.1) for 6 h at 37 °C. Cells were then washed and maintained in 500 μl (24-well) or 250 μl (48-well) of normal culture medium for 6–7 days at 37 °C. To determine HCV production activity, the amounts of HCV core protein in the culture medium and cell lysates were quantified with an enzyme-linked immunosorbent assay (ELISA) (Ortho® HCV antigen ELISA test, Ortho-Clinical Diagnostics, Japan).

Assay for activity of HCV genomic RNA replication

The RNAs (30 μg) transcribed from pSGR-JFH1/Luc and pSGR-JFH1/Luc-GND (Kato et al., 2005) were transfected into Huh7 cells (1.6×10^6 cells) by electroporation. Transfected cells in normal culture medium were immediately seeded into 48-well plates at 9.0×10^4 cells/well. Four hours after transfection, siRNAs were also transfected into these cells. After incubation for 2.5 days, cells were harvested and the luciferase activity in cell lysates was determined with the Luciferase Assay System (Promega). Since the luciferase activities of the JFH1/Luc replicon were ~400-fold higher than those of the JFH1/Luc-GND mutant replicon, background luciferase activity, which is independent of replication activity, was very low in our experimental conditions.

Immunofluorescence microscopy

Cells cultured on glass cover slips (in 24-well plates) were fixed in 1% formaldehyde-PBS for 1 h at 4 °C, permeabilized in PBS containing 0.1% Triton X-100 for 5 min, and washed twice with PBS. The cell monolayers were incubated with rabbit anti-vimentin antibodies (1:100) and mouse anti-HCV core protein antibodies (1:100) for 60 min at room temperature. After washing with PBS, the cells were incubated with Alexa488-conjugated anti-mouse IgG, Alexa594-conjugated anti-rabbit IgG, and DAPI (4′, 6′-diamidino-2-phenylindole) (Invitrogen) for 60 min at 4 °C. Coverslips were washed with PBS and mounted on glass slides. Immunofluorescence was visualized and quantitated with a confocal laser-scanning microscope (Axiovert 100M, Carl Zeiss) equipped with a LSM510 system (Carl Zeiss).

Acknowledgments

Huh-7.5.1 cells and Huh-7 cells were kindly provided by F. V. Chisari (Scripps Research Institute).

This work was supported in part by grants-in-aid from the Ministry of Health, Labor, and Welfare of Japan, and by grants-in-aid from the Ministry of Education, Culture, Sports, Science, and Technology of Japan.

References

Aizaki, H., Lee, K.J., Sung, V.M., Ishiko, H., Lai, M.M., 2004. Characterization of the hepatitis C virus RNA replication complex associated with lipid rafts. Virology 324 (2), 450–461.

Ariumi, Y., Kuroki, M., Abe, K., Dansako, H., Ikeda, M., Wakita, T., Kato, N., 2007. DDX3 DEAD-box RNA helicase is required for hepatitis C virus RNA replication. J. Virol. 81 (24), 13922–13926.

Bannasch, P., Zerban, H., Mayer, D., 1982. The cytoskeleton in tumor cells. Pathol. Res. Pract. 175 (2–3), 196–211.

Barba, G., Harper, F., Harada, T., Kohara, M., Goulinet, S., Matsuura, Y., Eder, G., Schaff, Z., Chapman, M.J., Miyamura, T., Brechot, C., 1997. Hepatitis C virus core protein shows a cytoplasmic localization and associates to cellular lipid storage droplets. Proc. Natl. Acad. Sci. U. S. A. 94 (4), 1200–1205.